MULTIPLE OBJECTIVE REACTIVE POWER PLANNING USING GENETIC ALGORITHMS

STEVEN M. SMALL

Your file Votre référence
ISBN: 978-0-494-33452-2
Our file Notre référence
ISBN: 978-0-494-33452-2

Multiple Objective Reactive Power Planning Using Genetic Algorithms

By

Steven M. Small, B. Eng.

A thesis submitted to the School of Graduate Studies

in partial fulfillment of the requirements for the

degree of Master of Engineering

Faculty of Engineering and Applied Science

Memorial University of Newfoundland

July 2007

St. John's Newfoundland and Labrador Canada

Abstract

Increased load demand can severely deteriorate the performance of a power system. Reactive compensation allocation is a common method to allow a power system to return to an acceptable performance level for an expected load increase. The reactive power planning problem (RPP) is used to determine the optimal placement of reactive devices for a set of objectives. The RPP is a large scale, multi-objective, highly constrained and partially discrete optimization problem that is very difficult to solve.

Heuristic optimization techniques have been used as a means to solve difficult optimization problems including many power system optimization problems. Heuristic techniques based on evolutionary strategies have been used to solve RPPs as they overcome many of the difficulties with classical optimization techniques. However, new multi-objective evolutionary computational techniques have shown the ability to consider an optimization problem's objectives independently for the determination of Pareto-optimal solutions.

A popular multi-objective evolutionary strategy called the *Non-Dominated Sorting Genetic Algorithm II* (NSGAII) is applied to a series of multi-objective RPP case studies in this research. The results from the case studies presented show that the tool is able to determine feasible, non-dominated VAr source allocation schemes that allow a system to operate safely under an assumed load growth.

Acknowledgements

I would like to thank and give my sincere gratitude to Dr. Benjamin Jeyasurya. His constant support, encouragement and guidance throughout this research experience were instrumental to my success at Memorial University of Newfoundland.

I would also like to thank my parents, Terry and Beryl, brothers, Sheldon and Aaron and of course Maggie Layman for their encouragement and support throughout my time as graduate student. I could not have gotten through it without them.

Special thanks and appreciation are given to the Natural Sciences and Engineering Research Council of Canada and to Memorial University of Newfoundland for the financial support, which made this research possible. Thanks are also given to the Faculty of Engineering at Memorial University for providing the resources to carry out this research.

Contents

List of Figures

List of Tables

List of Abbreviations and Symbols

BFGS	: Broyden-Flectcher-Goldfarb-Shanno formula
C_c	: Cost of reactive compensation devices per MVAr
e	: VAr source fixed installation cost
dec(str)	: Conversion of a binary string to its decimal representation
GA	: Genetic Algorithm
GBD	: General Benders Decomposition
I	: Current
I_c	: Cost of installing and Procuring VAr sources
N_{Branch}	: Number of transmission lines
N_{Bus}	: Number of system buses
N_{comp}	: Number of buses designated for VAr compensation
N_{PV}	: Number of PV buses
N_{Tap}	: Number of tap transformers
MO	: Multi-Objective
MOP	: Multi-Objective Optimization Problem
NSGAII	: Non-dominated sorting genetic algorithm-II
OPF	: Optimal Power Flow
P	: Active power
P_g	: Generator active power
P_l	: Power system active power load demand

P_{loss}	: Power system active power losses
p.u	: Per unit
Q	: Reactive power
Q_c	: VAr source reactive power
Q_g	: Generated reactive power
R	: Resistance
RPP	: Reactive Power Planning Problem
S	: Apparent power
S_{trans}	: Transmission line apparent power flow
SGA	: Simple Genetic Algorithm
V	: Voltage
V_{dev}	: Average load bus voltage deviation from nominal voltage
T	: Line transformer tap position
X	: Reactance
Y	: Bus admittance matrix
δ	: Angle of bus voltage
θ	: Angle of bus admittance matrix
£	: British pound

Chapter 1

Introduction

One of the great challenges of modern day power system operations is to meet constantly increasing load demand while maintaining reliable power delivery to their customers. This load demand increase coupled with the new deregulated operations environment are forcing existing generation, transmission and distribution infrastructures to support loads that they were never originally designed to handle. As a result of this, modern power systems are being operated in stressed conditions where their security is threatened. The recent blackout of August 2003 that affected many parts of Ontario, Canada and the North-East United States has shown the real need to develop solutions that enhance the overall security of the power system [1].

Simple solutions to facilitate power system load growth are to reinforce the existing transmission system and/or install new generators near major load centers. In most cases however, these solutions are not practical as the costs associated with the new transmission installations are tremendous and feasible generation sites may be too remote and too expensive to be effective.

In many cases, a simple solution that will allow a power system to safely handle a load increase is by allocating shunt reactive compensation devices at locations throughout

a system to provide sufficient local reactive power to system loads. This mitigates reactive power that must be produced by generators and transferred over the transmission infrastructure. By providing reactive power locally, the transmission system can be used more effectively as the negative effects of reactive power transmission are significantly reduced [2].

As compensation scheme installations can carry a substantial cost, it is desired to allocate them in a way that meets a range of operation criteria while minimizing costs. This multi-objective optimization problem (MOP) is known as the reactive power-planning problem (RPP) [3-10]. Although the objectives of the RPP (such as system voltage profile and reactor installation costs) vary depending on what a system planner deems important, in all cases the problem's mathematical formulation is exceedingly difficult to optimize. Over the last few decades the RPP has seen wide spread interest in the power industry as there are no widely accepted tools to solve the problem.

1.1 Overview of RPP Challenges

The RPP is a non-linear, non-convex and partially discrete MOP. For these reasons traditional optimization techniques based on non-linear, linear and integer programming have proven to be ineffective to adequately deal with all complexities of the RPP [3, 4]. While algorithms have been proposed based on these techniques, they are difficult to implement and require significant simplifying assumptions [4, 6, 7]. Coupled with these difficulties, classical optimization techniques are known to converge on non-

optimal solutions due to non-convex objective functions [12], and/or converge on infeasible solutions due to the treatment of discrete control parameters as continuous [3].

The greatest challenge associated with the RPP however, is that it can contain multiple objective functions for simultaneous optimization. Typically RPP algorithms simplify the problem by expressing it as single objective optimization problem where a master objective function is composed of a weighted sum of all desired objectives [3, 4, 6-8, 11]. The major problem associated with proposing a multi-objective problem as single objective problem is that an optimal solution may be highly dependent on how the weights are set [13]. This can be of great concern in cases where weights are arbitrarily assigned to objective functions.

A second problem associated with formulating a constrained MOP as a single objective problem is that the optimization procedure may determine a solution that is bordering on one or more constraint violations [13]. With regards to the RPP, it may be unwise to implement solutions that are close to violating constraints as a variety of potential system disturbances may push the system into an undesirable state of operation.

1.2 Research Objectives

The development of alternative optimization techniques such as genetic, evolutionary and particle swarm algorithms provide planners with a means to overcome many of the difficulties associated with the RPP problem [4]. These techniques have been applied to the RPP with weighted objective functions with good success [3, 4, 11].

However, research into exploiting the ability of these techniques to treat RPP objective functions independently has only recently begun. It is therefore beneficial to investigate the use of multi-objective optimization strategies for solving the RPP.

The purpose of the research presented in this thesis is to apply an algorithm based on a popular multi-objective genetic algorithm (GA) to solve the RPP while treating the selected objective independently. In comparison to other published approaches, it is easier to understand and provides a range of alternative solutions instead of a single potentially non-optimal solution. The principle goals of this research are summarized as follows:

1. Recognize the negative impacts of the remote transmission of reactive power and how reactive compensation can mitigate them.
2. Describe the general formulation of the RPP and outline some of the common tools used to solve it.
3. Study the concepts of the GA and evaluate the tool for solving optimization problems.
4. Outline and evaluate the concepts of multi-objective optimization.
5. Develop a tool that expands the concepts of GA optimization to incorporate true multi-objective optimization.
6. Apply the developed tool to suitable power system models in order to perform case studies that demonstrate the ability proposed algorithm to solve the RPP.

1.3 Thesis Summary

Chapter 2 presents important background on the concept of reactive power. The difficulties of remote reactive power transmission are described and illustrated using a 2 bus case study. Subsequently, the concepts and benefits of shunt reactive power compensation techniques are discussed. In chapter 3, a mathematical discussion of the RPP is presented along with three published techniques for solving the RPP. Chapter 4 presents the fundamentals of single objective GAs. The use of the GA will then be illustrated by applying it to a common power system optimization problem called the optimal power flow (OPF) using a study on a 7-bus power system. Chapter 5 will discuss the fundamental concept of multi-objective optimization, known as Pareto Optimality. Along with this discussion, the chapter will also outline a popular technique that expands the ability of a GA to treat MOP objectives independently. Chapter 6 will apply the expanded genetic algorithm to specific RPP test cases using a 6-bus power system and the IEEE 30-bus power system. Finally, chapter 7 will highlight some of the key contributions of the research completed in this thesis along with suggestions for future work.

Chapter 2

Reactive Power Transmission and Compensation: An Overview

2.0 Introduction

The remote generation and transmission of reactive power from load demand has a strong negative impact on power system operations. This chapter presents an overview of the challenges associated with the transmission of reactive power over a power system network. It will first illustrate the problems associated with reactive power transmission in section 2.2. Section 2.3 will give a fundamental understanding of shunt reactive power compensation and how it can be used to mitigate the negative effects of remote reactive power transmission. Section 2.4 concludes this chapter.

2.1 Reactive Power Transmission

It has been well established that the remote supply and transmission of reactive power to load centers can have an adverse effect on power system operations [14]. The flow of reactive power can cause many undesirable side effects such as an inadequate system voltage profile and unnecessary transmission congestion. Furthermore, in order to maintain certain voltage criteria, reactive power flow from a generator to a load can be difficult or impossible to accomplish.

To illustrate this fact, consider the lossless two bus system shown in figure 2.1.

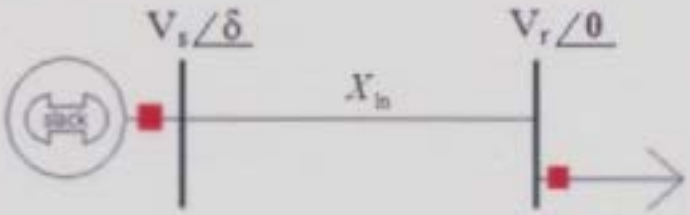

Figure 2.1: Two-Bus Radial Power System

It can be shown that the generation and load reactive power for the radial system is defined respectively by:

$$Q_s = \frac{V_s^2 - V_s V_r \cos\delta}{|X_{ln}|} \tag{2.1}$$

$$Q_r = \frac{V_s V_r \cos\delta - V_r^2}{|X_{ln}|} \tag{2.2}$$

where V_s is the generator terminal voltages, V_r is the load bus voltage, $|X_{ln}|$ is the magnitude of the line reactance and δ is the difference in voltage angle between the generation and load bus of the system. Since it is assumed that that the transmission line is purely reactive, the real power generation is equal to the load power and is defined by:

$$P_s = \frac{V_s V_r \sin\delta}{|X_{ln}|} \tag{2.3}$$

To observe the implications of these equations on reactive power flow, assume that V_s = 1 p.u, V_r = .95 p.u, $\delta = \pi/6$ rads and $|X_{ln}|$ = .1 p.u. Under these assumptions the sending reactive power, receiving reactive power and the active power are:

$$Q_s = 1.77 \text{ p.u}$$

$$Q_r = -1.27 \text{ p.u}$$

$$P_s = 4.75 \text{ p.u}$$

The negative value for Q_r is informing us that the load bus must have a means to *inject* reactive power into the transmission system in order to maintain the specified bus voltage while absorbing 4.75 p.u active power. The transmission line has become a sink for reactive power, demanding this power from both the generation system and the load bus for proper load bus voltage regulation. These results lead to the conclusion that for large load demand, reactive power does not have the ability to flow from the source to the load, even over a large voltage gradient [14].

A valuable technique widely used in industry to explore the relationship between power transfer and bus voltages is through the use of PV curves [14]. These curves are created by performing successive power flow studies on a system while increasing the

load levels on a specific bus set at a particular power factor. They provide a graphical way for understanding the effects of the transmission of reactive power flow on system voltages and maximum power transfer.

Figure 2.2 shows the PV curves for the system in figure 2.1 with three distinct power factor settings. In all the three cases it is apparent that the load bus voltage level decreases as load demand increases. The reason for this drop is the transmission reactance has its own reactive power requirement for carrying load power demand. This reactive requirement comes in the form of I^2X losses, which depress system voltages. Voltage depressions are more apparent with decreasing load power factor as increased transmission line currents are required to meet lagging load demand. This in turn causes larger transmission I^2X losses that further depress load voltages.

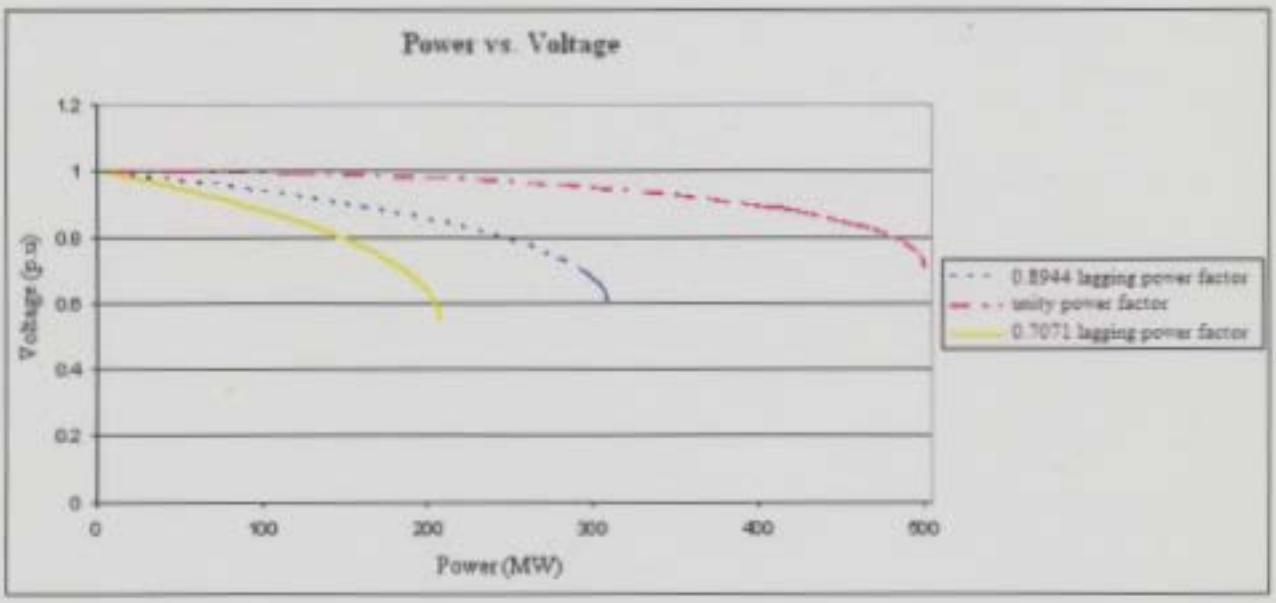

Figure 2.2: PV Curves for Various Load Power Factors

Another interesting point to note about figure 2.2 is the visualization of the amount of active power that can be transmitted through the transmission line. The maximum active power transfer is a direct result of practical power system operations, which typically requires bus voltages to be within ±5% the nominal voltage level. It is seen in figure 2.2 that the maximum amount of power transferred while maintaining the voltage requirement is exceedingly low for loads with high reactive demand. In fact, for this system, the maximum power transfer is only 45 MW for lagging power factor of 0.7071 and 90 MW for a power factor of 0.8944. In contrast, a maximum power transfer capability for a unity power factor load is about 280 MW. These results show that the remote transfer of reactive power is inefficient and unnecessarily congests the transmission system.

The results from above can be verified by observing the reactive power line losses and power demand as demonstrated in figure 2.3. When the load demand is low, reactive losses are not drastic as the line currents are low. However, as the load demand increases the line losses begin to dominate the system. Beyond the inflection point of these curves the reactive losses increase at an exponential rate, drastically reducing load bus voltage in a rapid fashion. These results properly correlate with figure 2.2.

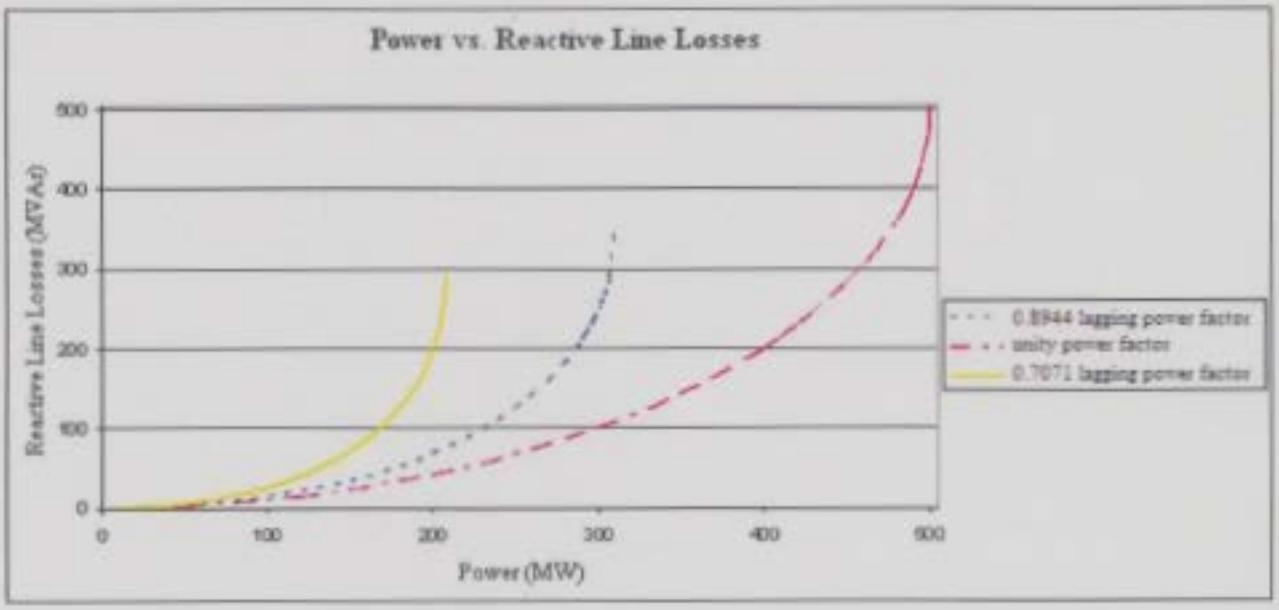

Figure 2.3: Transmission losses Versus Load Demand Power

2.2 Shunt Compensation for Reactive Power Flow Control

As was shown above, reactive power transmission has a negative impact on many aspects of power system operations. Without the proper control of reactive power a power system can be forced to operate in ways that threaten the systems voltages and its efficiency. The major objectives that the control of reactive power must satisfy to achieve reliable and efficient power system operation are [2]:

- Bus voltages should be within an acceptable limit to ensure that all equipment connected to the busses is operating in conditions they were designed for. Prolonged exposure to inadequate bus voltages can damage connected equipment
- Reactive power flow is minimized to reduce both active (I^2R) and reactive (I^2X) losses over transmission systems. This will ensure existing transmission infrastructure is utilized more efficiently.
- Increasing power system stability by utilizing the transmission systems more effectively.

By controlling the production, absorption and the flow of reactive power at all levels of the system, the above objectives for power system operations can be realized.

Local reactive power compensation is a convenient and common method to control reactive power flow to meet the mentioned objectives. Most compensation devices come in the form of switched inductor or capacitor banks that are installed in parallel to various load centers throughout a power system. Their purpose is to supply or absorb reactive power to loads such that the generation and transmission systems are unburdened by load reactive power demand. Reactive compensating devices such as these provide passive compensation that regulates voltages modifying system network topology [14]. While there are many forms of active reactive power compensating devices such as static VAr compensators and synchronous condensers, this thesis will focus strictly on passive compensation devices.

It is the complementary nature of inductive and capacitive loads that makes it possible to produce or absorb reactive power for power system loads locally. In order to understand this complementary operation in terms of reactive power, consider the inductor and capacitor with a potential across each device as seen in figure 2.4.

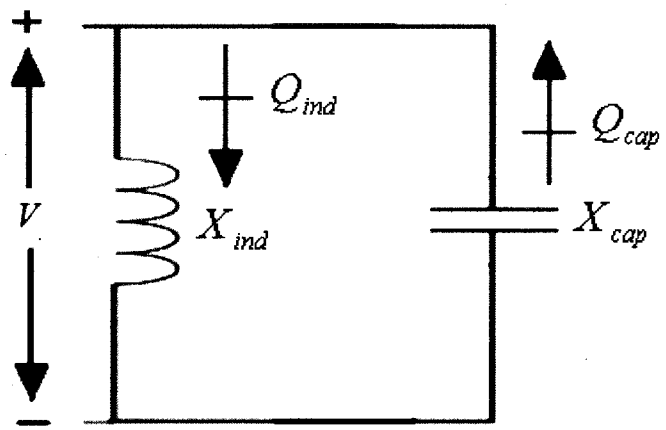

Figure 2.4: Reactive Power Direction of Capacitor and Inductor

The reactive power absorbed by a capacitor and an inductor in the *steady state* is given through the following equations respectively:

$$Q_{cap} = \frac{|V|^2}{|X_{cap}|} \tag{2.4}$$

$$Q_{ind} = \frac{|V|^2}{|X_{ind}|} \tag{2.5}$$

where V is the potential at the terminals of the reactive device, X_{cap} is the reactance of the capacitor and X_{ind} is the reactance the inductor. Since reactance is considered positive for

inductors and negative for capacitors the reactive power absorbed by the devices are positive and negative respectively. Reactive power can be modeled as flowing into an inductive load and as an injection into the capacitive load bus. This directional nature of reactive power flow for inductor and capacitor banks forms the basis for shunt reactive power compensation. Since the direction of reactive power for an inductive load is opposite that of a capacitive load, it can be viewed that the required reactive power absorption of an inductive load can be met through the capacitor banks' reactive power injection.

In power systems operation, the use of capacitor bank reactive injections near loads with high reactive absorbing demand is useful in preventing the remote transmission of reactive power. To demonstrate the effectiveness of such an installation, consider the addition of capacitor banks to the system in figure 2.1 as shown in figure 2.5. The load demand has been set to 250 MW at a lagging power factor of 0.8944 while the generator terminal voltage is set to 1 p.u. Without the use of any capacitive compensation the bus voltage is found to be 0.7980 p.u and the transmission line reactive loss is approximately 125 MVAr (see the plots in figure 2.2 and 2.3 respectively). These results show a heavily congested transmission line that in practical system operations would not be tolerable as the load bus voltage is well outside safe operation limits.

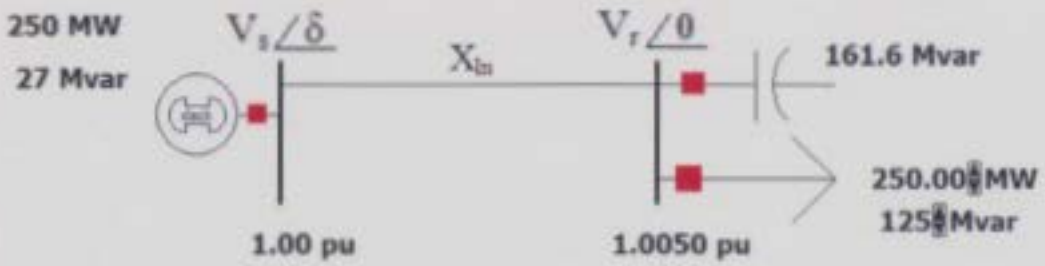

Figure 2.5: Capacitive Compensation Added to a Radial Power System

With the addition of a capacitor bank with a reactance of -j0.00625 p.u switched on at the load bus, a dramatic improvement in overall system performance is observed. As the capacitor bank is producing 161.6 MVAr, the complete 125 MVAr reactive demand of the load is being met locally by this local injection. Further, the additional 36.6 MVAr produced by the capacitor bank is injected into the system to ease the I^2X transmission line requirements for transport of the required active power as well as to reduce the generator's reactive power output. The effect of this local injection of reactive power is an increase in the load bus voltage by 0.2 p.u and a net decrease in transmission line reactive absorption by 62 MVAr. As the bus voltage is now within practical voltage limits it can be said that the transmission system is no longer congested and the increased active load demand can be met without any drastic changes in current generator and line configurations.

As stated above, most local reactive power banks contain blocks of capacitor reactance that can be switched on or off to adequately meet a wider range of load demand. This will help ensure that the voltage levels never exceed required voltages

during light loading while ensuring that proper levels of reactive power are injected into the system at various loading periods to maintain acceptable bus voltages.

To illustrate the usefulness of switched capacitor banks, consider again the system in figure 2.5 where this time the capacitor bank represents four blocks of switched capacitor reactance, all rated at –j0.02 p.u impedance. Figure 2.6 shows the PV curve for the system at a lagging power factor of 0.8944 with capacitor banks being switched on when the load demand causes the voltage levels to drop below 0.95 p.u. Clearly the capacitor bank switching action has extended the transmission capabilities to approximately 350 MW without any drastic system reconfigurations! It should be noted that this is assuming the transmission line itself is capable of handling 350 MW.

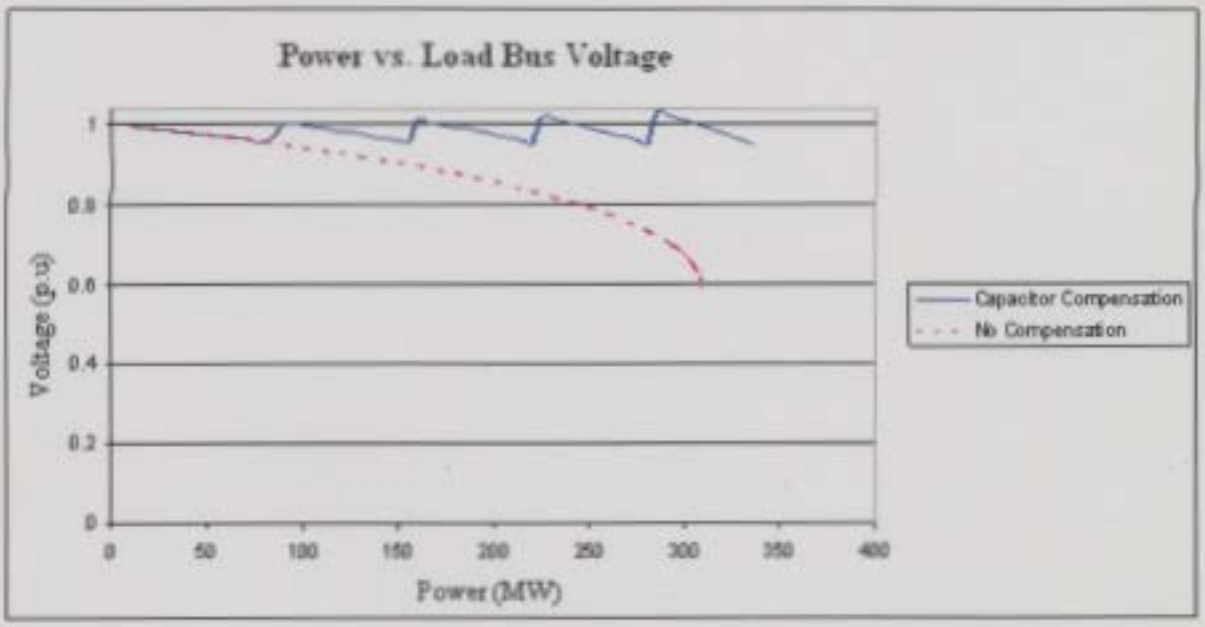

Figure 2.6: PV Curves for Switched Capacitor Bank

Looking at the transmission line MVAr losses with respect to load active power demand as shown in figure 2.7, the switched capacitor installation has drastically reduced the overall transmission reactive line losses. These results show that the capacitor bank installation can control reactive power flow thus increasing the effectiveness of current transmission systems.

Figure 2.7: Transmission Losses with Load Demand with Capacitor Compensation

As a point of interest, it should be noted that the losses still increase rapidly after a certain load level with reactive compensation. As a result of this, there is a limit to the effectiveness of capacitor bank installations beyond a certain loading level. This is especially apparent in figure 2.6, where the range of capacitor bank effectiveness is reduced when the load demand increases beyond a high loading point. The reason for

this is that the reactive demand of the transmission line is still excessive, even when capacitor reactive injection is being used.

2.3 Summary

This chapter provided the basic foundations on the difficulties of reactive power transmission. It was shown that reactive power transmission unnecessarily congests transmission systems which reduce the amount of active power that can be safely transported. It was also shown that system bus voltages throughout a system are negatively impacted by remote reactive power transmission. A simple 2 bus power system was used to illustrate the concepts regarding reactive power.

A cost effective and highly used approach to increase the efficiency of a power system was described. The use of local reactive power compensation devices that can be switched on or off can greatly increase the ability of a power system to meet a wide variety of load demands while insuring the system works within a specified voltage profile. This is an attractive option to power system planners as the costs associated with it are significantly lower then installing new transmission or generation systems to satisfy the increasing power demand.

Chapter 3

Optimal Reactive Power Planning

3.0 Introduction

Chapter 2 discussed the difficulties with the remote transmission of reactive power and the use of shunt compensation reactor banks to control reactive power flow. The use of reactive compensation devices has become a practical solution in controlling the flow of reactive power and to increase the reactive power reserves of the system. In most instances these devices are looked to as a solution to increase system voltages and decrease active transmission power losses over a planning horizon [3]. The planning horizon is a prediction of load growth that is known to potentially violate power system operation constraints.

The reactive power planning problem (RPP) is a common optimization problem faced by power system planners. It involves the allocation of reactive power reserves to meet a set of operational constraints while minimizing the costs associated with the

devices. As will be discussed below, the optimization of the RPP is exceedingly difficult for most optimization algorithms.

The organization of this chapter is as follows: section 3.1 will provide an overview on the formulation of the RPP as well as the challenges associated with solving it. Section 3.2 will discuss the major difficulties associated with solving the RPP with traditional optimization techniques. As background on the application of techniques to the RPP, section 3.3 will give a review of three published strategies that have been applied to solve the problem. The first technique based on problem decomposition will be presented in section 3.3.1 while the second and third technique, both based on heuristic optimization, will be presented in sections 3.3.2.1 and 3.3.2.2 respectively. Section 3.4 will give a summary of the chapter.

3.1 Reactive Power Planning Overview

The optimal placement of reactive sources throughout a power system is not a simple task. As there are no widely accepted tools to plan for reactive source installation, many planning procedures resort to a trial and error approach in order to determine the best site locations and allocation of reactive devices to meet a variety of objectives and constraints [4]. This procedure requires the planner to perform many power flow studies while varying reactive compensation settings and other pertinent system controls in order to ensure that the planned installations meet desired operation requirements. The trial

and error method is cumbersome and does not guarantee that that the proposed solution is optimal.

The RPP is a mathematical formulation that is intended to express the placement of reactive devices as an optimization problem in the *steady state*. As with many optimization problems, three major components need to be identified before formulating the RPP [12]. The first component is the identification of objective function(s), or the goals for optimization. Second, a set of controllable parameters need to be determined that have an impact on the selected objective function(s). Third, a set of operational constraints and conditions must be recognized in order to establish if the proposed solution is feasible.

These three components of an optimization problem can be described in the following standard mathematical form [15]:

Determine control parameter settings, $\boldsymbol{x} = (x_1, x_{2,\ldots}, x_n)^T$, that optimizes a vector of objective functions $F(\boldsymbol{x}, \boldsymbol{u}) = [\, F_1(\boldsymbol{x}, \boldsymbol{u})\ F_2(\boldsymbol{x}, \boldsymbol{u}) \ldots F_m(\boldsymbol{x}, \boldsymbol{u}) \,]$ (3.1)

subject to:

$G_i(\boldsymbol{x},\boldsymbol{u}) = 0$	$i = 1, 2 \ldots, z$	Equality Constraints	(3.2)
$H_i(\boldsymbol{x},\boldsymbol{u}) \leq 0$	$i = 1, 2 \ldots, p$	Inequality Constraints	(3.3)
$x_{iL} \leq x_i \leq x_{iU}$	$i = 1, 2 \ldots, k$	Control parameter bounds	(3.4)
$u_{iL} \leq u_i \leq u_{iU}$	$i = 1, 2 \ldots, v$	State variable bounds	(3.5)

where F($\boldsymbol{x}$, $\boldsymbol{u}$) is an array of objectives functions for *simultaneous* optimization, $\boldsymbol{u}$ is a state variable vector, x_{iL} and u_{iL} is the lower bound on each control parameter and state variable, x_{iU} and u_{iU} is the upper bound on each control parameter and state variable and m, n, z, p and v are the number of objective functions, control parameters, equality constraints, inequality constraints, control parameters and state variables respectively. Note that with regards to the RPP, the state variable vector consists of power system bus voltages and bus angles exclusively.

In order to optimally plan for reactive power compensation devices the components of standard optimization formulation need to be addressed. The following sections will discuss typical RPP optimization components found in literature for its formulation.

3.1.1 Reactive Power Planning Objective Functions

The role of objective functions is to mathematically express the goals of an optimization process. The objectives presented in this section represent the most common RPP goals. There are other less common objectives that will not be discussed in this thesis.

3.1.1.1 VAr Source Costs

The primary goal that is associated with all forms of the RPP is the minimization of costs for installing and procuring reactive devices for compensation [3-11]. Costs of reactive devices are typically broken down into two components: fixed installation costs and costs associated with purchasing devices. Installation costs are composed of the physical work that needs to be done and the cost of extra equipment required for the devices, such as switchgear and breakers. The combined costs of reactive sources can be modeled as follows:

$$I_c = \sum_{i \in N_c} \left(e_i + C_{ci} |Q_{ci}| \right) \tag{3.6}$$

where e_i is the cost of installation and additional equipment at bus i, C_{ci} is the cost per MVAr of the reactive compensator at bus i and Q_{ci} is the nominal rating (at 1p.u bus voltage) of the device in MVAr at bus i. Q_{ci} can be positive or negative depending on whether the compensation device required is inductive or capacitive.

3.1.1.2 Voltage Profile

Another possible objective is to minimize the deviation of power systems bus voltages from their nominal value [5]. There are a few purposes for using this objective. First, as described in chapter 2, reactive power transfer is highly dependant on system bus

voltage levels. By keeping load bus voltages close to their nominal values, less reactive power will be transferred to each load bus in the system [16]. This has the effect of reducing line currents which also reduces I^2R losses. As I^2R losses are a form of wasted power, this objective has a strong economical impact. The second reason for using this objective is that a power system that has its load bus voltages close to their nominal values is more resilient to voltage instability scenarios due to unforeseen contingencies such as a line outage [14]. The calculation of an average load bus voltage deviation, V_{dev}, used in this thesis is given by the following equation:

$$V_{dev} = \frac{\sum_{i \in N_{PQ}} |V_i - V_i^*|}{N_{PQ}} \tag{3.7}$$

where V_i is the actual bus voltage magnitude, V_i^* is the desired bus voltage magnitude and N_{PQ} is the number of load buses contained in the system.

3.1.1.3 Active Power Losses

While equation 3.7 indirectly controls the active power losses, many forms of the RPP include an expression to directly minimize wasted MW [3-11]. Like equation 3.7 this objective will help to ensure that the power system is performing economically. An expression for the overall active power losses accumulated in a power system is defined as:

$$P_{loss} = P_g - P_l \tag{3.8}$$

where P_g is the total active power produced by all system generators and P_l is the total active power load demand.

3.1.2 Reactive Power Planning Control Variables

As with the RPP objective functions, control parameters are dependent on what a planner believes will have an impact on system performance and the objective functions. Common RPP controllable parameters include the following [3-11]:

- Shunt compensator installations
- Generator terminal voltage levels
- Line tap changing transformers

These control parameters represent physical changes to the power systems operation and can be varied over their specified ranges.

Shunt compensation control parameters vary the amount of reactive power, Q_c, that the device will inject/absorb at nominal voltage (e.g. 1 p.u) at site installation busses. These control parameters are located and varied at any practical site location within the power system. Compensation devices, such as capacitors and inductors, commonly occur as blocks of reactive admittance and are purchased with *fixed* VAr ratings. Thus, reactor bank parameters are treated as discrete. While there are continuous forms of reactive compensation devices such as static VAr compensators and synchronous condensers, the costs associated with them tend to be significantly higher than fixed VAr sources [14].

As fixed reactor sources are a more commonly used reactive compensation device for cost reasons, this thesis will only focus on them.

Generator terminal voltages are another primary means to control system voltages. A machine's terminal voltage is controlled primarily through the use of automatic voltage regulators (AVR) [2]. The AVR is a closed loop control system that alters the synchronous machine's rotor field current to electromagnetically induce the desired voltage on the machine's stator winding. These control parameters are typically treated as continuous.

Tap transformers, while less commonly considered, are used to raise or lower the voltage on system buses when voltages lie outside their desired range. They alter voltages by mechanically moving the transformers' secondary tap position, T. Since these transformers have fixed tap positions, they are considered a discrete form of control.

3.1.3 Reactive Power Planning Constraints

Constraints contained within the RPP problem are put in place in order to ensure that the solutions obtained by solving the RPP are feasible for practical power system operations. Without these constraints in place, any optimization procedure that is done on the RPP could potentially lead to solutions that can leave the system in a stressed condition even after compensation has been applied. This section discusses typical operational constraints used in RPP formulation.

3.1.3.1 Equality Constraints

RPP equality constraints are represented by the power flow equations [16]. These equations define the physical link between scheduled generation and load demand and cannot be violated as they define the state variable conditions for a given system operating point. The power flow equations that govern the physics of the system are given in the following equations:

$$P_i = \sum_{j=1}^{Nbus} |V_i||V_j||Y_{ij}|\cos(\theta_{ij} - \delta_i + \delta_j) \qquad i = 1, 2, \ldots, N_{Bus} \qquad (3.9)$$

$$Q_i = -\sum_{j=1}^{Nbus} |V_i||V_j||Y_{ij}|\sin(\theta_{ij} - \delta_i + \delta_j) \qquad i = 1, 2, \ldots, N_{Bus} \qquad (3.10)$$

where P_i and Q_i are the active and reactive power bus injections at bus i, $|V_i|$ and $|V_j|$ are bus voltage magnitudes, $|Y_{ij}|$ is the magnitude of the element (i, j) of the power system's admittance matrix, θ_{ij} is the angle of the element (i, j) of the power system's admittance matrix, δ_i and δ_j are the bus voltage angles, and N_{Bus} is the number of system buses contained in the system.

3.1.3.2 Inequality Constraints

With respect to the RPP, inequality constraints define the tolerable limits on both state variables and equipment usage. Important limitations used in the RPP problem are as follows:

- Bus voltage magnitudes
- Generator active power limits
- Generator reactive power limits
- Transmission line apparent power limits

Bus voltage magnitudes must be held between a certain range in order to ensure that equipment is operating under design specifications, reactive power flow is controlled, line losses are reduced and voltage stability margins are within a desired range [14]. Allowable bus voltage levels depend on the nominal voltages that are applied to the bus. As an example, a typical tolerable voltage range for a 138kV bus is within ±5% of this value while buses with voltages of 345kV and over should be within ±10% [3].

Generation limits on active and reactive power are a result of the synchronous generators' design characteristics. These machines are rated in terms of maximum MVA at a specified voltage level and power factor which they can tolerate without overheating [2]. Synchronous machines have a maximum and minimum active power output that they can produce for efficiency and stability purposes [6]. Reactive power of a synchronous machine is limited primarily by the armature and field winding ratings.

Armature currents must be limited to reduce the windings' I^2R losses to ensure the machine does not overheat. Thus, for a given active power output, there is a limit on the amount of reactive power that can be produced or absorbed. The field current excitation, which controls the machine's reactive power output and voltage, must also be limited to insure that the machine rotor windings are not damaged due to excess heating.

All transmission lines have a limit for maximum MVA transfer, S_{trans}, to ensure the system is operated safely. One of the primary reasons for this is to help ensure that MW losses due to resistance in the line do not cause it to overheat. For instance, it is known that during high power system loadings, the power flowing over a transmission line can cause the transmission line to sag. If the line sag touches vegetation, a fault occurs, possibly leading to partial or system wide blackouts. This is believed to be one of the causes of the blackout of August 2003 [1].

3.2 Reactive Power Planning Challenges

The formulation of the RPP problem makes it quite difficult to solve using traditional optimization techniques. To show this, consider an example of the RPP where the goal of optimization is to minimize the costs of reactive sources (I_c) and the average load voltage deviation (V_{dev}) formulation as follows:

Minimize $F(\boldsymbol{x}, \boldsymbol{u}) = [\, I_c \; V_{dev}]$ (3.11)

Subject to:

$$P_i = \sum_{j=1}^{n} |V_i||V_j||Y_{ij}| \cos(\theta_{ij} - \delta_i + \delta_j) \qquad i = 1, 2, \ldots, N_{Bus}$$

$$Q_i = -\sum_{j=1}^{n} |V_i||V_j||Y_{ij}| \sin(\theta_{ij} - \delta_i + \delta_j) \qquad i = 1, 2, \ldots, N_{Bus}$$

$$P_{gi}^{\min} \le P_{gi} \le P_{gi}^{\max} \qquad i = 1, 2, \ldots, N_{PV} \qquad (3.12)$$

$$Q_{gi}^{\min} \le Q_{gi} \le Q_{gi}^{\max} \qquad i = 1, 2, \ldots, N_{PV} \qquad (3.13)$$

$$Q_{ci}^{\min} \le Q_{ci} \le Q_{ci}^{\max} \qquad i = 1, 2, \ldots, N_{Comp} \qquad (3.14)$$

$$V_i^{\min} \le V_i \le V_i^{\max} \qquad i = 1, 2, \ldots, N_{Bus} \qquad (3.15)$$

$$T_i^{\min} \le T_i \le T_i^{\max} \qquad i = 1, 2, \ldots, N_{Tap} \qquad (3.16)$$

$$S_{transi}^{\min} \le S_{transi} \le S_{transi}^{\max} \qquad i = 1, 2, \ldots, N_{Branch} \qquad (3.17)$$

where:

N_{Comp} is the number of buses that have been designated for possible compensation

N_{Bus} is the number of system buses

N_{Tap} is the number of tap transformers

N_{Branch} is the number of transmission lines

It is clear from the above formulation that in its mathematical form, the RPP is a partially discrete, large scale, multi-objective, non-linear, non-convex and highly constrained optimization problem. Classical techniques based on non-linear, linear and integer programming all have certain strengths associated with them that make them applicable for specific forms of optimization problems. However, the RPP formulation is too varied to make a single tool effective for adequately handling all properties of this problem.

The fact that the RPP is non-linear and non-convex poses a problem for using non-linear programming on the problem. While non-linear programming can deal with a problem's non-linearity, it works by taking derivatives to find the path of greatest ascent/descent. When this technique reaches a point in the search space where derivatives are equal to zero, an "optimal" solution is obtained. However, the technique's initial starting point coupled with function non-convexity can lead to local optimal solutions [4, 12]. There is no way to know whether the obtained solution is truly global optimum over the problem's entire search space.

Non-linear programming also suffers from the inability to deal with RPP's discrete control parameters such as reactor bank installations, hence discrete cost objective function, I_c. This is due to the technique's need of functional derivatives to obtain an optimal solution. As it is impossible to take derivatives at points of discontinuity, the only way to overcome the obstacle is to approximate the discrete control parameters as continuous. After the solution is obtained, control parameters are

then approximated to the nearest practical settings. This can lead to sub-optimal solutions or even infeasible solutions [7].

Integer linear programming is a tool developed for solving discrete linear optimization problems [17]. However, due to the non-linear nature of the RPP, this technique cannot be directly applied. While some RPP algorithms were developed using this technique, linearization assumptions of the RPP formulation are required [4]. Any assumptions that are made with the RPP lead to non-optimal solutions.

The RPP's multiple objectives create another significant challenge for any optimization tool. Multi-objective problems deal with the simultaneous optimization of a variety of objectives in order to determine the most effective control parameter settings. As a problem's objectives can conflict with each other, it is often impossible to obtain a particular set of control parameter settings to simultaneously optimize all selected objectives. This fact will be described in greater detail in chapter 5.

3.3 Review of RPP Optimization Techniques

The optimal placement of reactive compensation for power system operations is a highly researched topic and a vast amount of literature exists on various techniques aimed at solving the problem for similar problem formulations. This section will review three methods found in literature for solving the RPP. The discussed methods encompass both traditional and heuristic optimization techniques.

3.3.1 Decomposition Based Reactive Power Planning

Discussed in the previous section were the difficulties classical optimization techniques have with the RPP. Over the past few decades, decomposition techniques for large scale optimization problems were a highly sought after method to simplify difficult formulations so classical tools could be used more effectively [18]. As power system optimization problems are usually large scale, problem decomposition can improve computational efficiency and solution effectiveness by reducing the dimensionality of the overall formulation.

Perhaps the most common decomposition technique is known as the General Benders Decomposition (GBD) [18]. In order to apply the GBD, an optimization problem needs to be broken down into a master problem with one or more sub-problems. Generally speaking, the master problem is comprised of a mixed integer problem while the sub-problems are continuous. By doing this, different tool sets, such as mixed integer programming and linear programming, can be applied to applicable levels of the RPP problem.

Optimization via the GBD is done through the exchange of information between the master problem and the sub-problems. The master problem is comprised of a subset the control parameters that are usually discrete. During the iterative procedure, the master problem's control parameter settings are sent to the sub-problem level in order to optimize the remaining set of control parameters based on a different objective function. Any infeasibility that is determined at the sub-problem level is passed back to the master

problem's optimization tool to correct it by varying its parameters. This process is continued until optimization is complete at both levels of the GBD and no operational infeasibilities are present.

The GBD has been applied with varying success to large scale mixed integer power system applications such as the restructuring of transmission systems and the security constrained unit commitment problem (SCUC) [18]. There have been applications of the GBD to the reactive power planning problem [7-9].

The RPP can be broken down into the problem set seen by figure 3.1 for GBD application. The investment problem is treated as the master problem and it contains all discrete elements of the RPP. Since the investment problem can be made linear, its optimization is performed using mixed integer programming for the control of all discrete control parameters. The operations problem then accepts the proposed compensation scheme from the master objective problem. Linear programming can then be used on the remaining continuous control parameters by assuming the RPP constraints and objective function are linear [7].

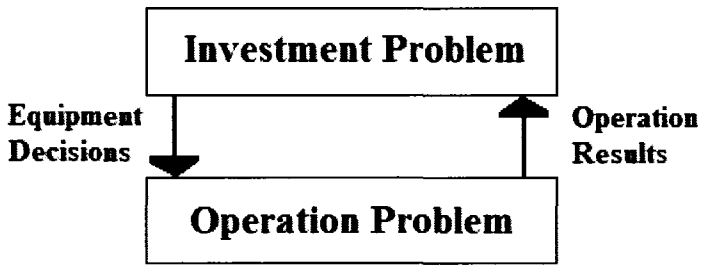

Figure 3.1: Decomposition of the RPP [9]

Although the decomposition technique allows the ability to use various optimization techniques at different levels of the RPP, it still may require linearization assumptions and the algorithm's complexity is very high. It has also been established that the GBD RPP based algorithms have a difficult time converging on solutions for large scale, practical power systems [4].

3.3.2 Heuristic Optimization Based Reactive Power Planning

Heuristic optimization techniques have been applied to give good results for solving the RPP problem as it searches for global optimal solutions. These techniques, which include the genetic algorithm (GA), evolutionary algorithm (EA) and particle swarm optimization (PSO), offer a robust means to solve optimization problems. They can be applied more readily to difficult optimization problems that classical techniques cannot be directly applied to [4]. The principles of the GA optimization technique will be discussed in chapter 4.

The following sections will discuss the application of two heuristic techniques found in literature for solving the RPP. The first is the EA for solving a single objective RPP, while the second uses the GA to solve a MO RPP.

3.3.2.1 EA Based RPP Optimization

The application of the EA to the RPP has resulted in a significant amount of published literature [3-5, 10-11]. The first published work for the application of EAs for solving the RPP problem was performed by Lai [3]. The goal of his work was to plan a shunt compensation scheme for a modified IEEE 30-bus test system and a practical UK 40-bus power system under different forecasted load levels using the EA. These load forecasts were proven to cause low bus voltages and high transmission losses.

The RPP objectives used in this study were the costs of reactive compensation devices (I_c) and the active transmission loss (P_{loss}). While these objectives define a multi-objective optimization problem, the problem was treated as single objective by weighting each objective appropriately and adding them together to form a master objective. The master objective function was defined by:

$$F(x,u) = I_c + h * d * P_{loss} \tag{3.18}$$

where h is the hourly cost of the active power transmission line losses in £/p.uWh and d is the duration period of the current load setting. Both d and h were used to ensure that the loss objective function was in units of £/year. It should be noted however, that the objective functions themselves are still in different units as the VAr source cost is in units of £ while the loss cost is in units of £/year. However, as the planning horizon is considered over one year only, the overall objective function is considered to be in units of £.

To demonstrate the effectiveness of the EA for solving the RPP, an example of the results obtained from the work is briefly presented here. In this example, the IEEE 30-bus system was used where the overall real and reactive load demands were assumed to be 5.668 p.u and 2.524 p.u respectively. Results obtained from the test procedure are given with respect to a base apparent power of 100 MVA.

In order to explore the load expansion system operation violations, a base case power flow was performed for a predefined generation schedule and tap transformer settings (set to 1.0 p.u). The results of this base case power flow showed that the expected load demand caused violations for bus voltages and generation reactive power limits. The violations, as shown in table 3.1, put the power system in an undesirable state of operation.

Table 3.1: List of Violated Constraints for a Modified IEEE 30-bus system

Bus	9	10	12	14	15	16	17	18	19	20
V_i **(p.u)**	0.945	0.909	0.940	0.901	0.893	0.910	0.897	0.870	0.863	0.872
Bus	21	22	23	24	25	26	27	29	30	-
V_i **(p.u)**	0.879	0.880	0.866	0.849	0.855	0.811	0.880	0.829	0.799	-
Bus	1	2	5	8	11	13	-	-	-	-
Q_{gi} **(p.u)**	-0.402	0.496	0.952	1.479	0.281	0.439	-	-	-	-

The minimization of equation 3.6 was performed through the control of 14 distinct parameters. The control parameters and type used for the RPP were as follows:

- Four reactive compensation installation sites on buses 6, 17, 18 and 27.
- Four tap transformers, located on branches (6,9), (6,10), (4, 12) and (28, 27).
- Six generator bus voltages found at buses 1, 2, 5, 8, 11 and 13.

Finally, the master objective function was evaluated for control parameter setting using the assumed objective function constants:

- The hourly cost (h) of active power losses is 6000 £/(p.uWh).
- The duration time (d) was given as 8760 hours.
- Installation costs of reactive power sources (e_i) are £1000.
- Cost of procuring a reactive source (C_{ci}) is 3,000,000 £/(p.uVAr).

The control parameter results of the EA optimization procedure are found in table 3.2. The tap settings found in this table give the transformer tap setting position. They represent the desired increase or decrease on each of the devices' secondary winding voltage. The reactive power source installations represent the amount of VArs the capacitor bank will inject into the system at a nominal voltage of 1p.u. Based on the author's test case discussion, the optimization process performed by the EA managed to determine control parameter settings that removed all the observed constraint violations. Hence, a feasible solution was obtained.

Table 3.2: EA Based Optimal Control Parameter Settings

Generator Bus Voltages (p.u)						
Bus	1	2	5	8	11	13
V_i	1.05	1.022	0.973	0.959	1.050	1.050
Tap Transformer Settings (p.u)						
Branch	(6, 9)	(6, 10)	(4, 12)	(28, 27)	-	
T_i	1.05	1.1	1.1	1.1	-	
Reactive Power Source Installations (p.u)						
Bus	6	17	18	27	-	
Q_g	0.198	0.229	0.133	0.196	-	

The costs associated with the EA's reactive compensation installation scheme and yearly losses are found in table 3.3. In order to show the strength of the EA approach to the RPP as a cost saving tool, a second method to determine compensation scheme was discussed using the Broyden-Fletcher-Goldfarb-Shanno (BFGS) technique [12]. The BFGS is based on the classical non-linear optimization technique based on Newton's method that seeks to optimize by taking first and second order derivatives of functions in order to guide the algorithm's search direction.

Table 3.3: EA and BFGS Solution Costs for One Year Planning Horizon

Method	**Cost of installation (£)**	**Cost of losses (£)**	**Overall costs (£)**
EA	12252262	2272000	14524262
BFGS	12342665	3217000	15559665

It is apparent from these results that the heuristic EA technique has significantly outperformed the BFGS optimization method with an overall cost savings of £1,035,403, assuming the system operates under this loading condition for a one year duration. Lai suggested that the reason for the differences in costs could be attributed to EAs ability to

perform a global search, while the BFGS, like any calculus optimization procedure, got caught on local optima. In this case, the costs associated with a local optimal answer are significant and should be avoided.

3.3.2.2 Genetic Algorithm Based RPP Using Multiple Objectives

Recent interest in Pareto optimization has sparked a significant amount of research in the area of engineering multi-objective optimization. This interest is due to Pareto optimization's ability to consider objective functions independently so any natural trade-off that occurs between objectives can be observed. This trade-off region shows that for true MOP, the simultaneous optimization of objective functions is not possible based on the selected control parameters. Pareto-optimality is described and illustrated in chapter 5 of this thesis.

Pareto-optimality was applied to the RPP problem by Begovic et al. [10]. A bi-objective GA was used to approximate the true Pareto frontier between the installation cost objective and the active power losses for both a transmission system and a distribution system. The Pareto optimization algorithm for the transmission RPP was performed on a simple 4-bus system (see figure 3.2). To show the strength of the GA Pareto optimization method, the results of the transmission line optimization found in the study are presented here.

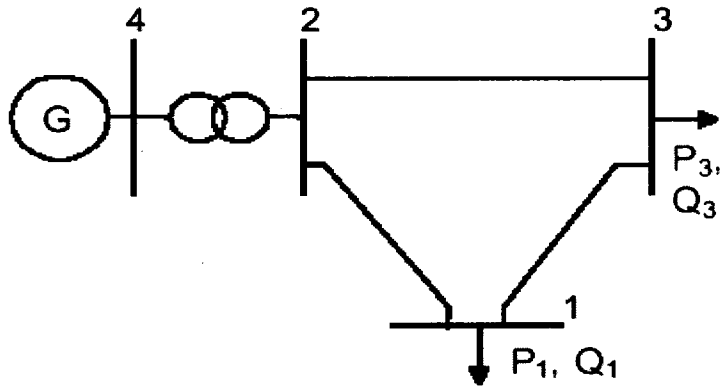

Figure 3.2: 5-Bus Test System Used for Pareto Optimization [10]

In the study only the reactive compensation MVAr installations were used as control parameters in this study. Two potential reactive compensation locations were selected at bus 1 and 3 as they help to satisfy the local reactive power demand. These control parameters were treated as discrete, where the step size for each parameter was assumed to be 1MVAr. Installation costs for reactive compensation were neglected and the costs for the devices was assumed to be 10$/KVAr.

The results of the GA based Pareto optimization technique used in the paper is found in figure 3.3. In this figure the *x*-axis represents the *total* active transmission losses while the *y*-axis represents the *combined* reactive power compensation installation sizes for both buses 1 and 3.

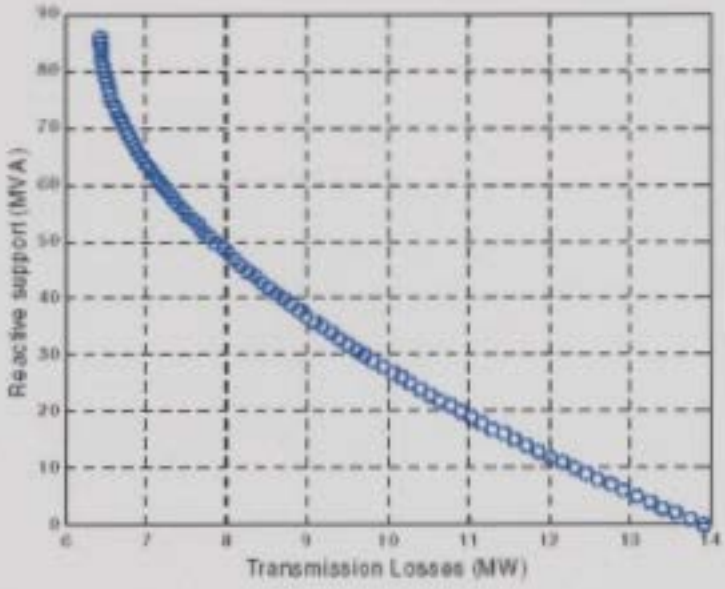

Figure 3.3: Pareto Frontier for GA Multi-Objective Optimization [10]

The decaying trend shown in this figure represents the non-dominated solutions of the Pareto frontier, where each solution is no better then the next in terms of objective optimization. As expected from the discussion in chapter 2, more reactive power compensation installations results in less severe active transmission losses, while line losses increase with less compensation.

The benefits of using the Pareto approach for solving the RPP is also evident in figure 3.3. This figure clearly shows that the objective values conflict with each other as mentioned above. Because of this conflicting relationship, the creation of a single objective can lead to solutions that are not optimal for either objective. The trade-off region gives a planner the ability to select a solution from a range of Pareto optimal solutions. Thus, engineering judgment can be used to select a solution based on some other criteria not used in the RPP formulation.

3.4 Summary

This chapter discussed the fundamentals of the reactive power planning problem and the difficulties in solving it. Along with this discussion three published techniques for application to the RPP were presented. One method was based on problem decomposition for the application of different traditional tool sets. The two other methods presented were based on based on heuristic optimization methods. From the literature on all three discussed methods, heuristic optimization is the most viable strategy for solving RPPs.

Heuristic techniques are highly sought after as a realistic means to solve difficult optimization problems as they have proven themselves to be flexible and robust by design. The two examples of evolutionary heuristic techniques presented above show promising results. One reason that these methods are applicable to the RPP is that heuristic techniques have been shown to handle discrete elements of an optimization problem. Second, they have the ability to perform a global search of the problem space which gives it the ability to obtain better results than classical techniques.

Heuristic optimization techniques can be implemented to produce a close approximation to the Pareto-optimal set. This has its own merit as the RPP objective functions are known to conflict with each other. Thus, there exists no unique answer to simultaneously minimize all objectives. This is an attractive alternative as other criteria, such as ease of solution implementation and engineering judgment can be used to determine the best solution out of an optimization problem's Pareto set.

The next chapter will discuss and give a detailed description of genetic algorithms as they will be used in this thesis to solve multi-objective RPPs in the Pareto-optimal sense. Genetic algorithms will be shown through two optimization problems to be an effective tool to locate optimal solutions.

Chapter 4

Genetic Algorithms

4.0 Introduction

Genetic algorithms (GA) were first developed in the 1960's by Holland [19] as a unique tool geared towards optimization problems. It also provided the foundations for the development of other popular evolutionary programming techniques such as evolutionary algorithms (EA) and particle swarm optimization (PSO). The GA is a heuristic optimization technique that is inspired by biological functions. Heuristic optimization methodologies are, by definition techniques that use intelligent guesswork to obtain solutions instead of using some form of pre-established formula and/or methodology. The heuristic property of the GA comes from the algorithms' attempt at artificially emulating Darwin's theory of evolution [20]. Unlike a trial-and-error heuristic method, the GAs use of evolution as its decision making framework allows the algorithm to make intelligent assessments about promising areas of an optimization problem's search space in order to locate an optimal solution. While the GA does not guarantee the

true optimal solution, it can provide near optimal results with a significant reduction in computational time [19].

Since the initial development of the GA, significant research has been done involving its application to challenging engineering optimization problems including applications to the RPP [3, 4, 10]. This research has lead to different variations of the original *simple genetic algorithm* (SGA) [13] including the development of additional algorithm operators that allow it to cope with true multi-objective problems. A popular multi-objective GA will be described in chapter 5.

The objective of this chapter is to provide the fundamental concepts regarding GA based optimization. It should be noted here that while many forms of GA coding exist such as integer and continuous, this thesis will focus on *binary* genetic algorithms only as described below. This chapter is organized as follows: Section 4.1 will provide an overview of a single objective GA. Along with this overview, common GA operators will be discussed. Section 4.2 describes the advantages of GA based optimization. Section 4.3 will illustrate the GA optimization process using a simple mathematical optimization problem. The development and application of the GA to the optimal power flow (OPF) [21] for a seven bus power system will be illustrated in section 4.4 to give better insight into GA based optimization. Section 4.5 will conclude the chapter.

4.1 Overview of the Genetic Algorithm

Biological evolution primarily consists of three important functions that serve to strengthen a species' ability to cope within its surrounding eco-system. These functions are natural selection, genetic recombination and genetic mutation. Combined together and allowed to occur over many generations, they help ensure that a given population *evolves* important traits that allow a species to remain an intrinsic part of their living environment. In much the same way, Holland proposed to incorporate the mechanics of evolution into an algorithm that would adapt dynamically to feedback from information stored within a population of solutions [19]. The overall goal of this algorithm is to *evolve* optimal solutions from a randomly generated set of solutions of size N.

How can it be possible to use evolution to solve intricate optimization problems? Certainly one of the keys to the GAs success is in its artificial representation of a biological population. The GA uses a population of string structures to represent possible solutions to a given problem - analogous to living creatures. These string structures, called chromosomes, are comprised of an array of *genes* which represent control parameters for an optimization problem. Genetic traits are imprinted on each chromosome's genes to represent control parameter settings. Thus, the genetic traits, or the *DNA* of a chromosome actually represents a specific solution to an optimization problem.

As an example of artificial genetic representation, consider the following optimization problem:

Minimize $z = x\sin(4x) + 1.1y\sin(2y)$ (4.1)

Subject to:

$$0 \le x \le 10 \quad (4.2)$$

$$0 \le y \le 10 \quad (4.3)$$

where x and y are assumed to be continuous over their respective range.

For this optimization problem, each chromosome contained within the population is comprised of two genes which are used to store the x and y control parameter settings. With binary genetic algorithms, control parameter settings are not stored as base-10 numbers. Instead, set string lengths of 1's and 0's are used to represent them. This representation is shown in figure 4.1.

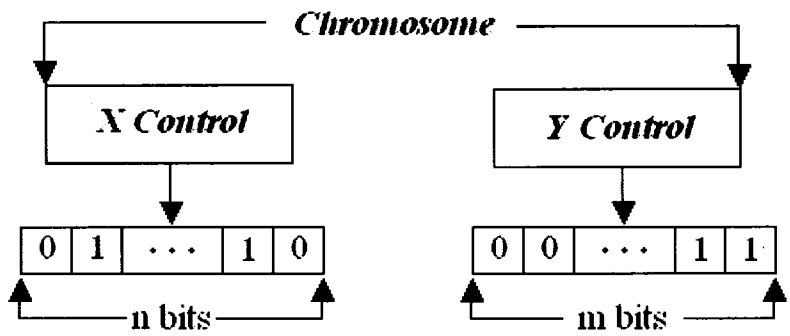

Figure 4.1: Binary Chromosome Representation for Control Parameters

Modeling of control parameters as a binary set of strings is important to most of the GAs evolution operators. However, these strings are not particularly useful for numerically determining how fit each chromosome is. As the GA uses an optimization problem's objective function as a *fitness landscape* [20], binary control strings must be

decoded into a base-10 number in order to evaluate each solution's fitness. For the case of the continuous control variable optimization problem above, an equation that can be used to convert a binary number into a decimal number is given as:

$$u_i = u_i^{\min} + \left(\frac{u_i^{\max} - u_i^{\min}}{2_i^{l_i} - 1} \right) dec(str_i) \tag{4.4}$$

where u_i is the decimal representation of a binary encoded parameter, u_i^{min} and u_i^{max} is the minimum and maximum allowable value of a parameter respectively, l_i is the number of bits used to represent the parameter and $dec(str_i)$ is the conversion of a binary to decimal number. The quantization of the conversion is highly dependant on the number of bits chosen to represent the control parameters. Using more bits will allow for a more precise representation of continuous control parameters.

As an example of decoding binary control parameters, consider the chromosome shown in figure 4.2. In this example each control parameter is coded using 6 binary digits. Using equation 4.4 and the inequality constraints set by equation 4.3 it can be found that the decoded decimal value for the x and y control parameters are 7.7778 and 3.6508 respectively.

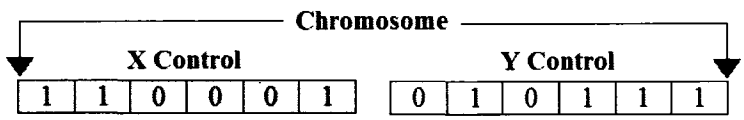

Figure 4.2: Example of a Two Variable Chromosome

After the decoding of binary data for each control parameter is complete it is possible to evaluate the chromosomal fitness. By evaluating an optimization problem's objective function for chromosomes' gene settings, it is possible to have a relative scale of how fit each chromosome contained in a population is with respect to each other. The mapping of the chromosome in figure 4.2 is seen in figure 4.3.

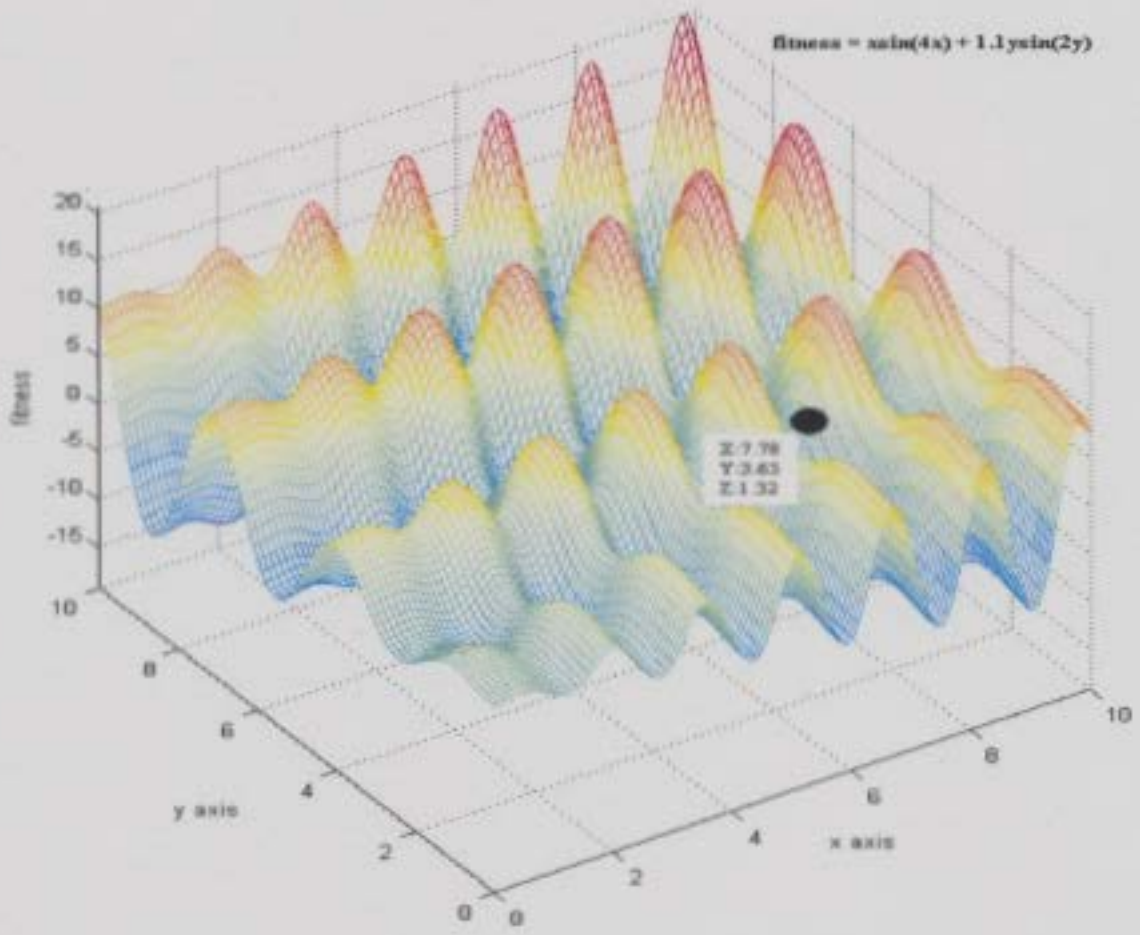

Figure 4.3: Mapping of Chromosomes into the Fitness Landscape.

In the natural world, it is known that weak members of a species population have a difficult time coping with the challenges of their environment and most often perish.

However, strong members have the traits that allow them to thrive. Natural selection rewards the strong individuals with a greater chance to pass on their genetic traits to future generations. It also helps to significantly increase the probability that poor genetic traits contained in weak individuals are not passed on to subsequent generations. This insures negative characteristics that impede the coping ability of an individual are eliminated from the gene pool. Similarly, the GA rewards solutions with large relative fitness. The reward is the opportunity to pass on their strong genetic traits into future generations.

There have been many proposed methods to emulate natural selection such as roulette wheel and stochastic selection [22]. However, the most flexible and easily used strategy is known as tournament selection. Tournament selection is a probabilistic operator that randomly selects two chromosomes from the population and pits them into competition with each other. The winner of the tournament is the chromosome that has the largest fitness value. An example of a tournament is shown in figure 4.4. The tournament selection operator performs this task N times in order to create a *mating pool* of fit *parents* of size N.

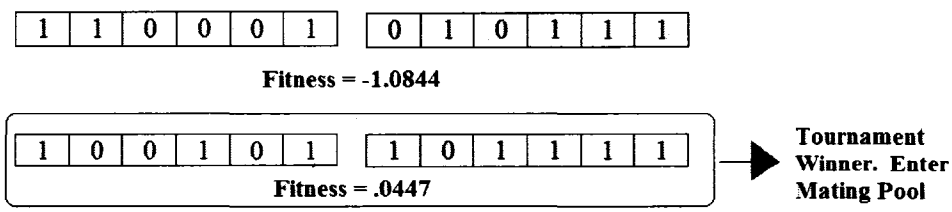

Figure 4.4: A Tournament between Two Competing Chromosomes.

Members of the mating pool are given the opportunity of passing on their genetic information on to the next generation. Just like natural reproduction, subsequent children consist of a mixture of genetic information from two parents. As tournament selection weeds out poorly fit chromosomes, children are expected to consist of only strong genetic material. This results in an improved overall fitness of the new population versus the old population.

There have been many techniques to emulate *genetic recombination.* Common probabilistic methods include uniform, single point and two point crossover, with the latter being highly used [23]. The two point crossover operator works by first selecting two parents from the mating pool at random. These parents are then aligned as shown in figure 4.5 such that like control parameters are paired together. The operator gets its name from the fact that two crossover points are selected at random to mark which part of each parent's genetic data will get transferred to the two children. For instance, child 1's x control setting is composed of the first two bits of parent 1, the third and fourth from parent 2 and the fifth and sixth from parent one. Child 2's x control settings will be the inverse, taking its first two bits from parent 2 and so on. The parents used to create the children are then discarded from future consideration. This process of creating children is continued until there are N children. The next generation chromosomes consist of the newly created child population.

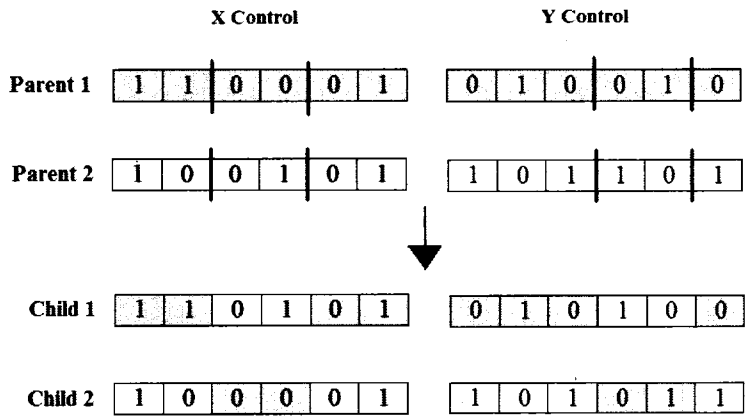

Figure 4.5: Two Point Crossover for Two Variable Optimization Problem.

It should be noted here that the process of fusing genetic information to create children occurs within the GA with a high probability. However, the algorithm does not guarantee that new children are created. Instead, the selected parents are sometimes passed through the operator and enter the next generation unaltered.

The final evolutionary function implemented in the GA is based on genetic mutation. In the natural world, it is fairly common for children to contain traits that neither parent nor any member of a population has. These new genetic traits may help or hinder the ability to adapt well to its surrounding environment. If these traits are beneficial to child's survival, natural selection helps to ensure that they are passed on to future generations of the species. If however, the traits adversely affect the child, natural selection should help ensure that these traits never make it into the next generation.

Like the GAs selection and recombination operators, the *mutation* operator is probabilistic. After the children are created and have replaced the parents as the next

generation of solutions, this operator goes through each child's binary digits and converts them from a 0 to a 1 or vice versa with a low probability. A low probability is used to ensure that the search is based on evolution, not pure randomness [20]. However, even with a low probability, this operator helps to ensure that the entire fitness landscape has the opportunity of being searched. An illustration of mutation is shown in figure 4.6. In this figure, a gene is examined by the mutation operator where the second bit is converted from a 0 to a 1.

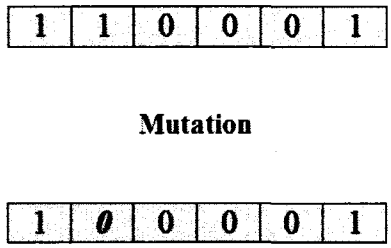

Figure 4.6: An Illustration of Mutation.

Most GAs uses an additional operator known as *elitism* [20]. While this operator is not based on evolutionary functions it does serve to enhance the overall effectiveness of GA based optimization. In many cases of GA evolution, the best obtained from previous generation may be lost due to the probabilistic nature of the GAs operators. This operator is used to keep track of the best (elite) solution obtained so far during the algorithm's search. If it is found that all members of the subsequent generation have lower fitness then the elite solution, the operator will replace a randomly selected solution in the population with it. If there is a member of the population with a higher fitness than

the current elite member, then that member becomes the new elite member. This operator is known to ensure faster optimization convergence.

Using these operators iteratively over many generations, optimal or near optimal solutions can be obtained. A simple GA algorithm can be coding in any programming language by following the flow chart as shown in figure 4.7. Note that the loop contained within this flow chart will be called the main evolution loop in this thesis.

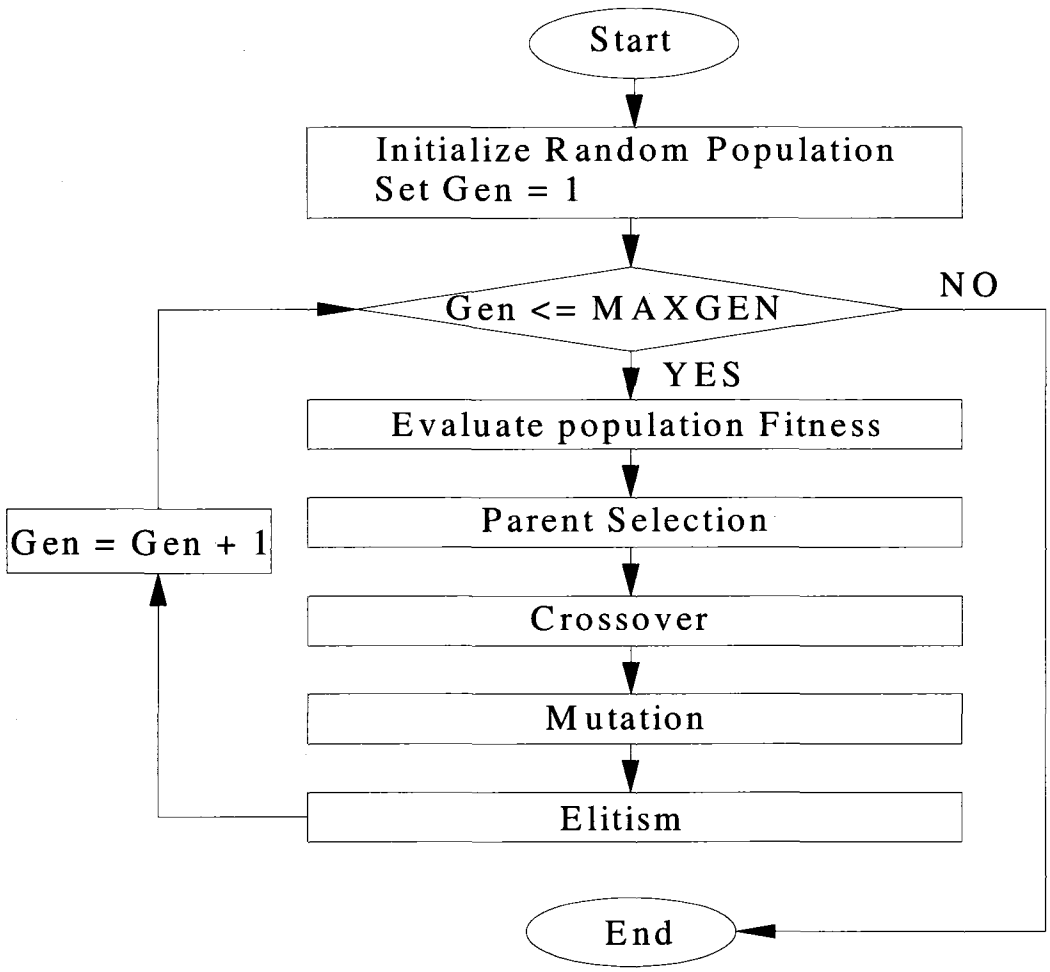

Figure 4.7: A Simple Genetic Algorithm Flow Chart

4.2 Benefits of GA Based Optimization

Evolutionary programming strategies, such as the GA, have several significant advantages over classical optimization methods and trial and error processes. These advantages include the ability to avoid local optima convergence and not needing to simplify portions of the optimization problem's formulation.

GAs begin an optimization procedure by creating a randomly created population of solutions to the optimization problem. For this reason, as soon as the optimization procedure begins, the GA uses feedback from the strengths and weaknesses of the population to get an idea of good regions of the fitness landscape. These regions are rigorously explored by the GA by using the evolutionary operators as described above [19]. This has the advantage over the non-linear programming techniques which require a starting point to perform its search, often leading to local optimal solutions. Further, the use of evolutionary heuristics allows the GA to perform a guided search while a brute force trial and error approach requires variables to be changed without any benefit from the exploration of the fitness landscape. Thus, the GA requires less computational time then the brute force approach.

Unlike non-linear optimization techniques that require the existence of first and second order derivatives and continuous control variables, the GA makes no assumptions about an optimization problem's formulation. As a result of this, the GA has the ability to be applied to challenging optimization problems to which classical techniques cannot be applied. One reason for this is that GAs work with the coding of the control

parameters, not the parameters themselves. By using different techniques to decode control parameters into base 10 numbers, it is possible to incorporate discrete control parameters into the GA. A second reason is that the GA guides its search by using payoff obtained from the optimization problem's objective function, not derivatives or other auxiliary knowledge [19].

4.3 An Example of Mathematical GA Optimization

As a visual aid to see the evolution of an optimal solution with GAs, consider again the optimization problem represented by equations 4.1 to 4.3. By inspection, it is apparent that the global minimum solution is located approximately at x = 9.0 and y = 8.6 which results in z = -18.5.

The results presented here based on GA optimization were obtained by coding the GA from figure 4.7 using MATLAB 7.0 [24]. Table 4.1 lists the important GA settings used for this example. The crossover and mutation probability values were chosen based on recommendations given in [20]. These values allow good exploration while not resulting in a random search due to excessive mutation.

Table 4.1: GA Settings for Minimization of 4.3

X Control Parameter Bit Number	12
Y Control Parameter Bit Number	12
Population Size	20
Generation Number	100
Mutation Probability	0.001
Crossover Probability	0.85

It should be noted here that in order to minimize an objective function using a tournament selection based GA, the optimization problem's objective function needs to be transformed in order to map negative values into higher fitness values for the GA chromosomes. A simple way to accomplish this is to simply multiply equation 4.1 by -1 [20].

Figure 4.8 shows a contour plot of equation 4.1. Contained within this contour plot is a randomly generated set of chromosomes (solutions), where each is represented by a black asterix. It is clear from this figure that the chromosomes are well spread out over the fitness landscape to allow the GA to locate promising areas of the search space. Good solutions within this population are located in or near blue portions of the contour plot.

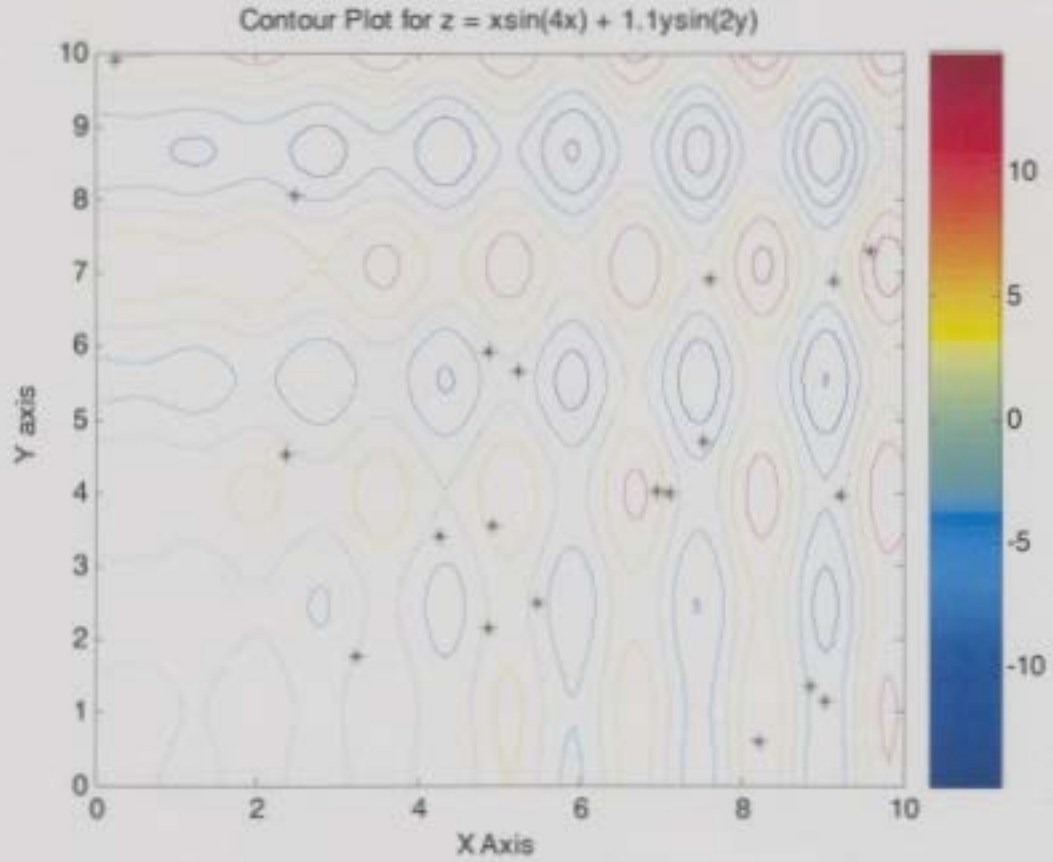

Figure 4.8: Contour Plot of the Initial Population

With the random population created, the GA then enters the main evolution loop for 150 generations. Figure 4.9 shows the elite solution versus the generation number. Clearly, early in the GAs optimization process better solutions are obtained very rapidly with each generation. After generation number 27, the GA has converged on a final solution as the subsequent generations do not lead to any further improvement in the overall best solution.

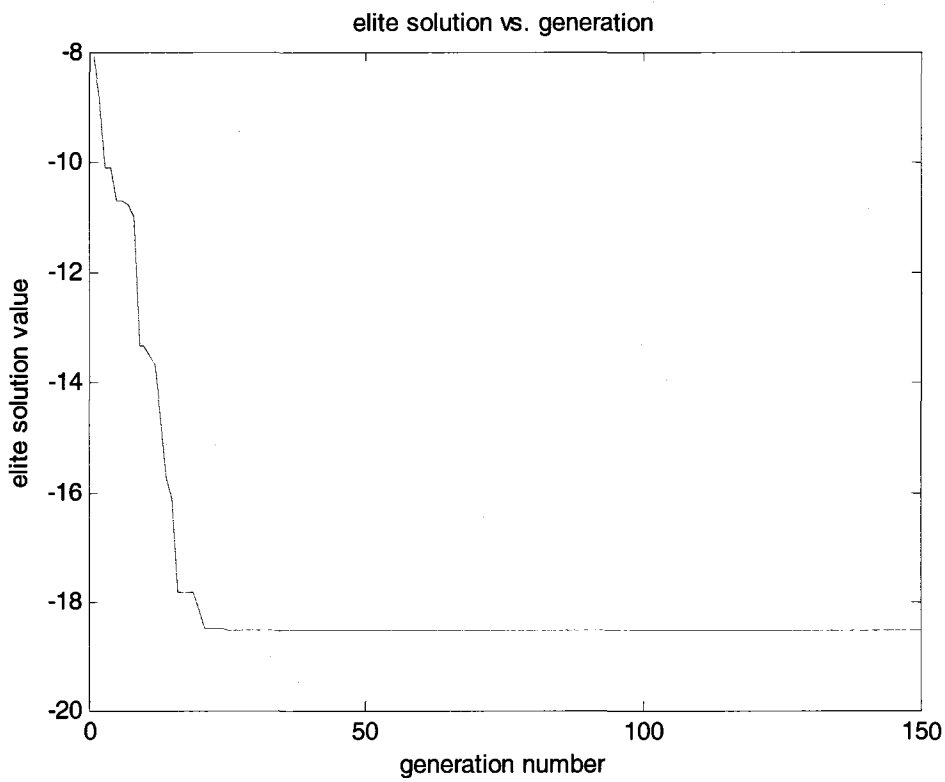

Figure 4.9: Progress of the Elite Solution for each Generation

The resulting population at the end of the GAs iterations is shown in figure 4.10. This figure shows a significantly improved population in terms of fitness. As expected, the entire population is biased towards the upper right quadrant of the contour plot as this is where the global optimal solution is located. For this reason, many of the population's chromosomes are scattered on or close to the global optimal point. Note the figure does not show all 20 chromosomes as many of the chromosomes are copies of each other.

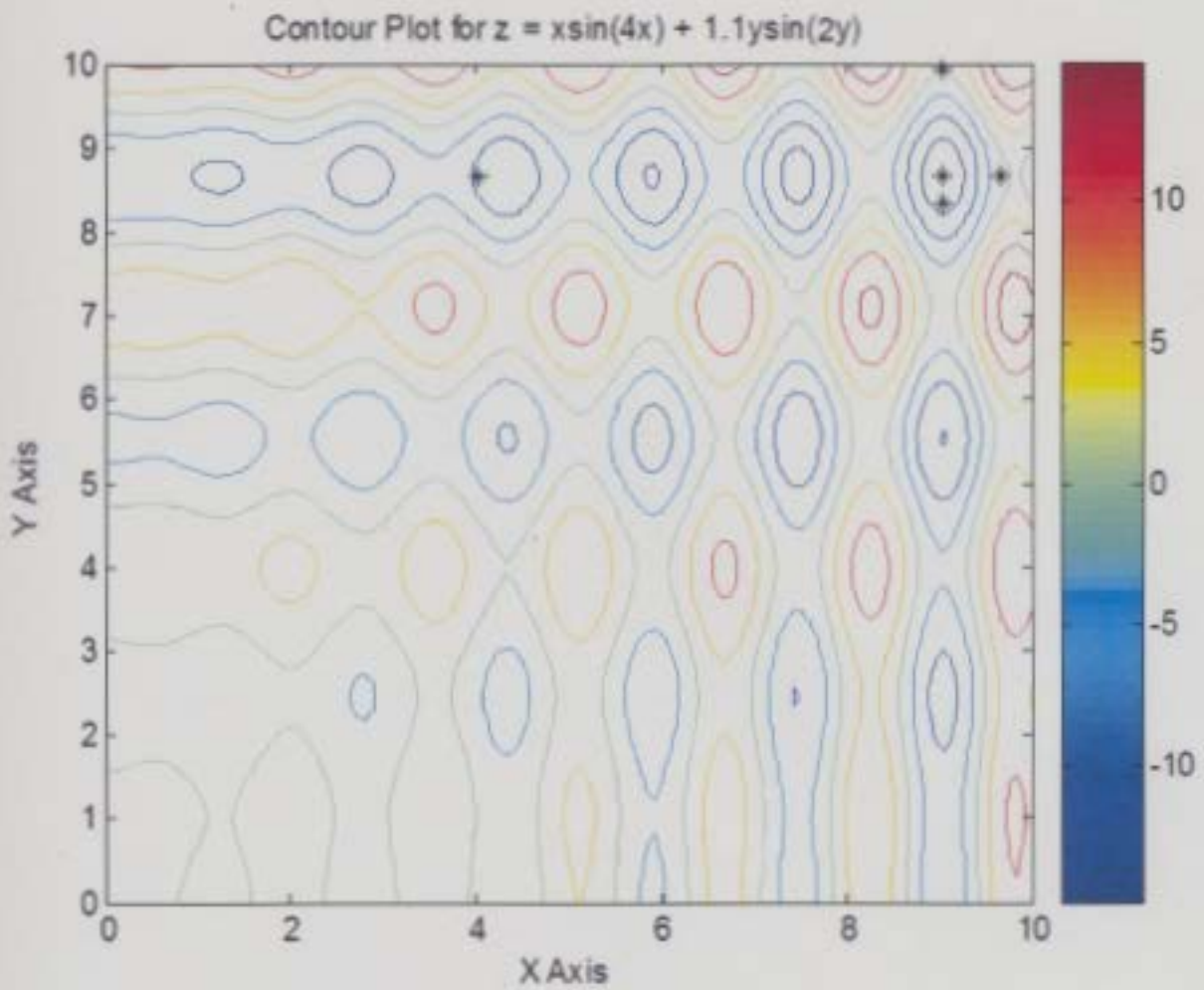

Figure 4.10: Contour Plot of the Final Population

The resulting elite solution's control variables and objective evaluation value are shown in table 4.2. As a comparison, a non-linear programming technique based on Newton's method [12] was used to solve the same optimization problem. Using MATLAB's *fmincon* optimization function along with the initial search point x = 9 and y = 9 the optimal solution also shown in table 4.2 was obtained.

Table 4.2: Two Control Parameter Optimization Results

Method	X Control Variable	Y Control Variable	Objective Evaluation
GA Method	9.0390	8.6682	-18.5547
Newton's Method	9.0379	8.6740	-18.5540

While these results are near identical, it is important to understand that Newton's method obtained the optimal solution because inspection of the surface plot for equation 4.1 gave the proximity of the global solution. If a different starting point was chosen, the algorithm would converge on a local optimal solution.

4.4 Application of the GA to Optimal Power Flow

The purpose of the OPF is to determine a generation schedule that meets a load demand while meeting a wide range of operational constraints. In its most general formulation the OPF is a single objective, large scale, non-convex optimization problem. It has been widely used by electric power utilities since its origin in the 1960's [21]. Many techniques have been used to solve the OPF, including linear, non-linear and evolutionary programming with good success [25, 26]. The objective of this section is to evaluate the effectiveness of the GA optimization technique for a 7-bus OPF problem. Simple power system models will be used to illustrate the effectiveness of the Genetic Algorithm approach.

4.4.1 Optimal Power Flow Formulation

Most power system generators require the consumption of fuel to provide electrical power. The objective function of the OPF reflects these costs. A common representation for a generator fuel cost in dollars per hour is given by the following quadratic equation:

$$C_{P_{Gi}} = \alpha_i + \beta_i P_{Gi} + \gamma_i P_{Gi}^2 \tag{4.5}$$

where P_{Gi} is the active power output from generator i and α_i, β_i, and γ_i are the cost coefficients for generator i.

The sum of all the generator costs represents the total operational costs, in dollars per hour, for providing the required active power to load demand. Thus, the OPF objective function for minimization is expressed as:

$$f(P,u) = \sum_i (\alpha_i + \beta_i P_{Gi} + \gamma_i P_{Gi}^2) \tag{4.6}$$

where P is a vector of generator power outputs.

As with the RPP, the OPF is bounded by many operational constraints. The optimization equality constraints are representative of the OPF's equality constraints. The optimization inequality constraints represent limits on each generator active and

reactive power outputs, bus voltages and transmission line and transmission line MVA transfers.

Using the objective function and the operational constraints, the OPF can be expressed in the following optimization form:

Minimize $f(P,u) = \sum_i (\alpha_i + \beta_i P_{Gi} + \gamma_i P_{Gi}^2)$

Subject to:

$$P_i = \sum_{j=1}^{n} |V_i||V_j||Y_{ij}|\cos(\theta_{ij} - \delta_i + \delta_j) \qquad i = 1, 2, \ldots, N_{Bus}$$

$$Q_i = -\sum_{j=1}^{n} |V_i||V_j||Y_{ij}|\sin(\theta_{ij} - \delta_i + \delta_j) \qquad i = 1, 2, \ldots, N_{Bus}$$

$$P_{gi}^{min} \le P_{gi} \le P_{gi}^{max} \qquad i = 1, 2, \ldots, N_{PV}$$

$$Q_{gi}^{min} \le Q_{gi} \le Q_{gi}^{max} \qquad i = 1, 2, \ldots, N_{PV}$$

$$V_i^{min} \le V_i \le V_i^{max} \qquad i = 1, 2, \ldots, N_{Bus}$$

$$S_{transi}^{min} \le S_{transi} \le S_{transi}^{max} \qquad i = 1, 2, \ldots, N_{Branch}$$

Note that the above equality and inequality constraints are fully discussed in chapter 3.

4.4.2 GA-OPF Objective Function and Fitness Function

Unlike section 4.3, which dealt with an unconstrained optimization problem, the OPF is heavily bounded by operational constraints to keep the system inside safe

operational limits. Constrained optimization using non-linear optimization techniques introduce the concept of penalty factors to discourage the algorithm from obtaining infeasible solutions [21]. Similarly, GAs can use penalty factors to reduce the fitness of infeasible solutions to discourage the GA from searching infeasible portions of the search space [3, 20, 25, 26].

A simple way to apply the penalty factor approach to GA optimization is to simply augment the problem's objective function with weighted penalties for any constraint violation that occurs for a member of the GAs population. This leads to the following GA-OPF objective function:

$$F(P,u) = f(P,u) + \sum_{i \in N_v} \lambda_i (H_i - H_i^{\lim})^2 \tag{4.7}$$

where λ_i represents the user defined weight of the penalty associated with the ith constraint, N_v defines the set of constraint violations, H_i is the value of the ith violated constraint parameter and H_i^{lim}, depending on whether the violation is over or under the parameters constrained limit, is the minimum or maximum tolerable value.

As with the minimization problem in section 4.3, the OPF requires a transform to map small or negative objective function values into high fitness. This again can be accomplished by multiplying equation 4.7 by -1 to yield a GA-OPF fitness function:

$$Fitness(P,u) = -f(P,u) - \sum_{i \in N_v} \lambda_i (H_i - H_i^{\lim})^2 \tag{4.8}$$

4.4.3 7-Bus GA-OPF Test Case and Results

The goal of the OPF for the 7-bus, 5 generator power system [27] seen in figure 4.11 is to minimize generator fuel costs while adhering to power flow equations, specified branch flow (MVA), bus voltage magnitudes, generator reactive power and slack generator active power limits. The limits, fuel cost coefficients and the system parameters are found in Appendix A. The total load demanded by this system is 760MW and 130MVAr. This system has 9 controllable parameters in total: 4 generator active power output variables and 5 generator bus voltage magnitude variables. The reference bus is located at bus 7.

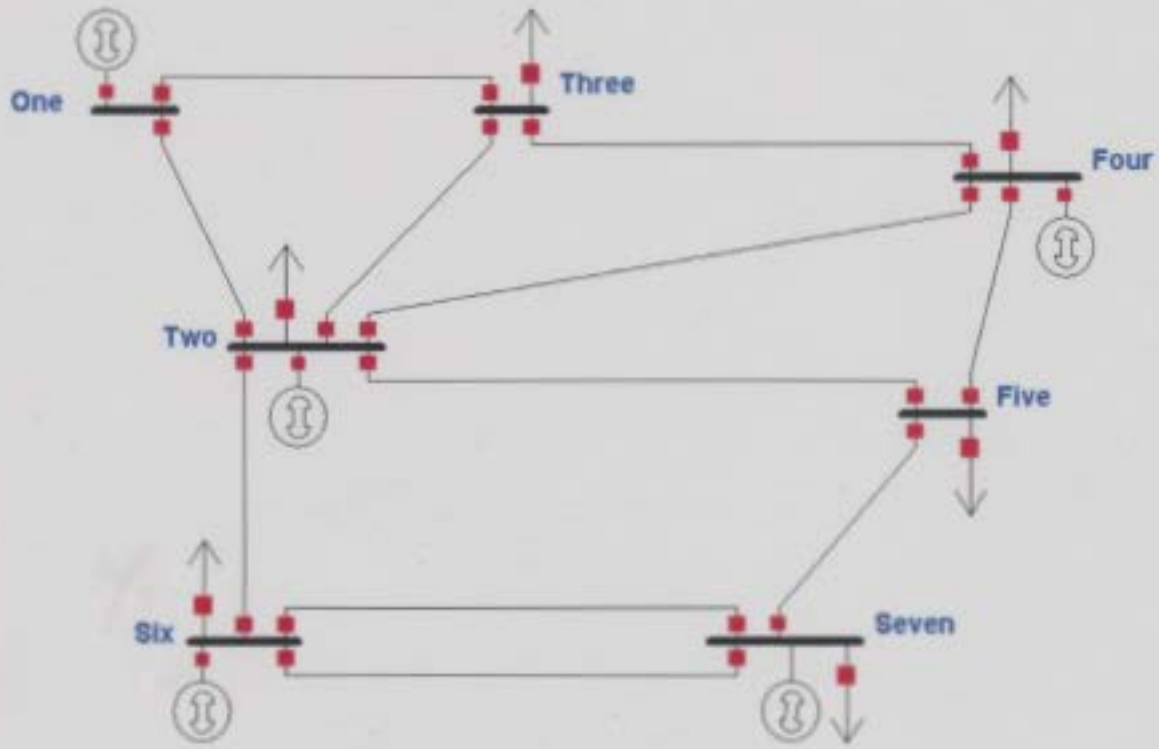

Figure 4.11: Single Line Diagram for the 7-Bus Power System

This test case was coded in MATLAB 7.0 and ran on a 3.0GHz Pentium 4 PC with 512MB of RAM. A MATLAB based power systems toolbox known as MATPOWER [28] was used to perform the required power flows for chromosomes in the population in order to determine the value of the reference bus' active power output and to determine all constraint violations for fitness evaluation. The following table shows important GA parameters used in this study.

Table 4.3: GA Settings for Minimization GA-OPF Test Case

Generator Power Parameter Bit Number	12
Generator Voltage Parameter Bit Number	8
Population Size	30
Generation Number	200
Mutation Probability	0.001
Crossover Probability	0.85

The GA-OPF results presented in table 4.4 are based on the best and worst case of 10 runs to show that the GA's heuristic approach can lead to different solutions. Each GA-OPF run required approximately 115 seconds of processing time. As a comparison to the GA-OPF technique, the results of MATPOWER's Newton based OPF technique is also presented in the table. The table shows each of the control variable set points along with the slack generator output and the overall cost to operate the system for the required load demand. None of the results presented in this table had any constraint violations.

Table 4.4: GA-OPF and MATPOWER OPF Case Study Results

Bus	***Unit***	**Best Run GA-OPF**			**Worst Run GA-OPF**			**MATPOWER OPF**		
		|V| (p.u)	*P (MW)*	*Cost ($/hr)*	*|V| (p.u)*	*P (MW)*	*Cost ($/hr)*	*|V| (p.u)*	*P (MW)*	*Cost ($/hr)*
1	*1*	1.05	100.00	1155.50	1.049	100.00	1155.50	1.05	100.00	1155.50
2	*2*	1.048	161.71	1656.12	1.041	160.05	1646.55	1.048	160.56	1646.91
4	*3*	1.037	127.73	1275.34	1.028	130.04	1294.22	1.037	128.36	1280.48
6	*4*	1.041	205.13	1997.08	1.031	205.42	1996.35	1.047	205.72	2001.88
7	*5*	1.024	173.04	1595.87	1.011	172.07	1587.69	1.024	172.95	1595.14
		Total	767.61	7679.91	Total	767.58	7680.31	Total	767.59	7679.91

From the table it is apparent that there are slight differences in the results of best and worst case GA results. This is due to different initialized populations being biasing to different but promising areas of the search space from run to run. However, the overall costs associated with the two cases are almost identical. Also, the best case solution of the GA-OPF is identical in terms of cost as MATPOWER's optimal solution. While these results obtained do not show that the GA is any better at solving the OPF, it does show that its optimization technique gives acceptable results and is applicable to difficult optimization problems.

4.5 Summary

This chapter provided an overview of key genetic algorithm concepts along with the benefits of using it for solving difficult optimization problems. As the GA does not require any auxiliary knowledge of an optimization problem, such as the existence of functional derivatives, the GA is applicable to many types of optimization problems to which techniques such as non-linear programming cannot be easily applied.

Through a highly non-linear mathematical optimization problem, the GA was shown to provide a global approach to optimization. Its performance for this application was excellent as it was able to provide the global optimal solution. The optimization problem consisted of multiple local optimal solutions that caused non-linear programming strategies to locate sub-optimal solutions. The only reason the non-linear technique managed to find the global solution was the inspection to find close proximity of where the global solution was located. In most optimization problems, the ability to visually determine where the optimal solution is located is impossible due to dimensionality.

This chapter also proved the applicability of the GA to power system applications. It was demonstrated that the GA could locate an optimal solution for a 7-bus OPF. While the results were not superior to Newton's OPF method, the results show the GAs ability to solve difficult optimization problems. As was shown in chapter 3, the RPP contains discrete control parameters. The GA's ability to cope with discrete control parameters

and its ability to deal with highly non-linear optimization problems as illustrated in this chapter, potentially make it a good fit for solving the RPP.

The only downfall to the GA with respect to non-linear programming was the longer processing time required for solving optimization problems as was shown with the GA's application to the OPF. Extended processing time inherently limits the GAs applicability to problems that *do not* require near instantaneous solutions. The processing time expense for planning type problems is greatly offset by the GA's ability to perform global searches and its use of discrete control parameters.

Chapter 5

Multi-Objective Optimization: A Genetic Algorithm Approach

5.0 Introduction

Chapter 3 alluded to the fact that, in general, MOPs contain a set of optimal solutions instead of a single solution. These solutions are called Pareto-optimal and show the inherent trade-offs that occur between competing objective functions [10, 13, 29, 30]. In the absence of any auxiliary information, it is impossible to say that any Pareto-optimal solution is better than the others. A good optimization procedure should seek out as many of these optimal solutions as possible in order to select the best solution based on other criteria.

Strategies based on classical optimization techniques have been proposed to solve MOPs [10, 13, 29, 30]. These strategies involve assigning a weight to each of the objective functions based on relative importance and summing them together to create a single objective function [10, 13, 29, 30]. With this formulation, a single solution can be

obtained. However, multiple solutions can be obtained by applying an optimization algorithm many times while assigning different weights to the objective functions. While this method is intuitive, there is no guarantee that the algorithm will produce Pareto-optimal solutions due to the local search of classical techniques [13]. A second problem that is common to a weighting scheme is that each objective may be of different units, such as time or money. It may be difficult to transform these objective functions such that all objective functions are composed of the same units [13].

Over the past few decades, many MO optimization tools based on evolutionary strategies have been proposed. These techniques are well suited to search out multiple optimal trade-off solutions as they operate globally on a collection of points instead of relying on a starting point like classical optimization techniques. Thus, a range of optimal solutions can be obtained with just one run of the algorithm. Just as important however, is their ability to treat a problem's objectives independently [30]. This removes the issues associated with the aggregate objective function technique as described above.

The aim of this chapter is to discuss a powerful and popular extension of genetic algorithms that allow them to effectively solve MOPs. This chapter is organized as follows: Section 5.1 will discuss the concept of Pareto-optimality for minimization problems. 5.2 will overview a state-of-the-art technique known as the *Non-dominated Sorting Genetic Algorithm-II* (NSGAII) for MOP optimization. Section 5.3 will illustrate the effectiveness of the NSGAII for a simple bi-objective optimization problem. Section 5.4 will give a summary of this chapter.

5.1 Pareto Optimality

As stated above, most MOPs do not allow for a single solution to optimize all desired objective functions. As many practical problems are defined to contain conflicting objective functions, trade-offs between objectives are apparent. For instance, consider an optimization problem that has two objectives (called bi-objective), where one objective is the minimization of costs to create a product and the other is the minimization of time required to produce a product. Assuming that spending more money allows a plant to purchase more efficient machinery, the overall time to create a product should be lower. However, if less efficient machinery is purchased to save money, the time expected to produce should be higher.

The conflict that exists between the mentioned objectives is clearly shown in figure 5.1. From the figure's objective space, it is apparent that solution X (requiring a greater cost) and solution Y (requiring greater time) have attributes that, in a sense make them optimal. Clearly, there is a trade-off here; an increase in the optimality of one objective degrades the quality of the other objective. Thus, the only way to actually say that one solution is better then the other is to use other criteria not defined in the MOP.

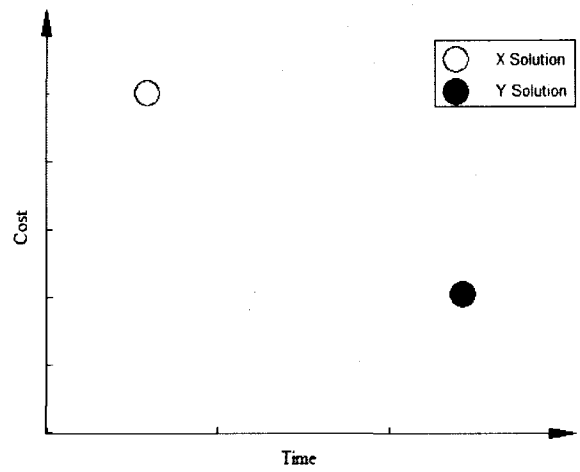

Figure 5.1: Trade-off between Two Solutions, X and Y

While the above example illustrated that it may be impossible to determine a solution to optimize all objectives, the question still remains as to what is an optimal solution is for a MOP. A key to this lies in the definition of solution *domination*. By definition, a solution X, is said to dominate a solution Y, if both conditions 1 and 2 are true [30]:

1. The solution X is no worse than solution Y in all specified objective functions.
2. The solution X is strictly better than Y in at least one of the specified objective functions.

If either of the above conditions is violated, solution X does not dominate solution Y. In fact, if we consider the above conditions with respect to solution Y instead, it may be determined that Y dominates X.

To illustrate the concept of domination, consider a minimization bi-objective optimization problem with only two solutions, X and Y, as illustrated in figure 5.2. It is

evident in this figure that solution X has a lower value with respect to both objective functions. In no way is solution Y optimal in any sense. Since solution X meets both conditions for domination of solution Y, it is said that solution X dominates solution Y. In fact, if other solutions did exist and were located in the region highlighted in this figure, the solutions would also be dominated by solution X.

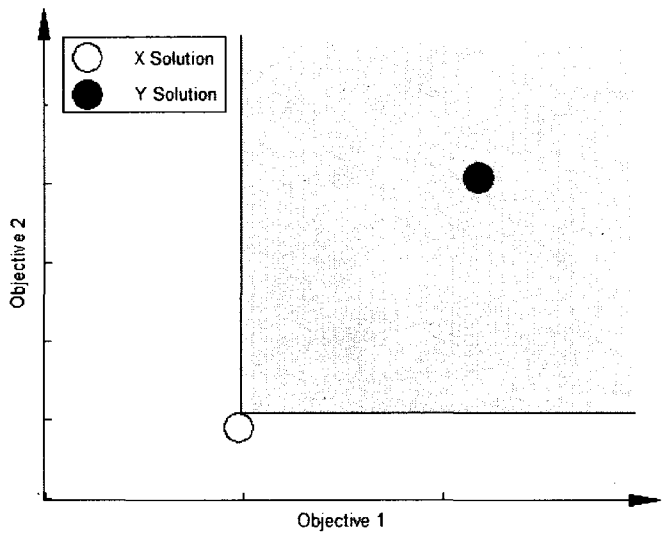

Figure 5.2: A Depiction of Solution Domination.

Dominated solutions are not of interest for MOPs. The reason for this is that there are other solutions in the objective space that better facilitate the optimization of all required objectives. Instead, MOP optimization is focused on obtaining *non-dominated* solutions, which are in direct contrast to dominated solutions.

A non-dominated solution is defined as any feasible solution such that there does not exist *any* other feasible solution contained in the entire objective space that is strictly better than it for *all* objectives. These solutions are called Pareto-optimal, after the Italian

economist Vilfredo Pareto (1848-1923) [13]. For a given MOP, the collection of Pareto-optimal solutions is called the Pareto front. As described above, Pareto-optimal solutions are in a sense optimal.

Continuing with the cost-time example from above, figure 5.3 shows the optimal trade-offs that occur between the two objective functions. The solid line represents the Pareto-optimal frontier that contains all the non-dominated solutions for the MOP. Clearly the front is showing that as we increase the optimality of time we decrease the optimality of cost, however no solution within the front is better with respect to both objectives. This line also shows that any objective space solution that is above and to the right of the front is dominated by at least one solution contained in the Pareto frontier.

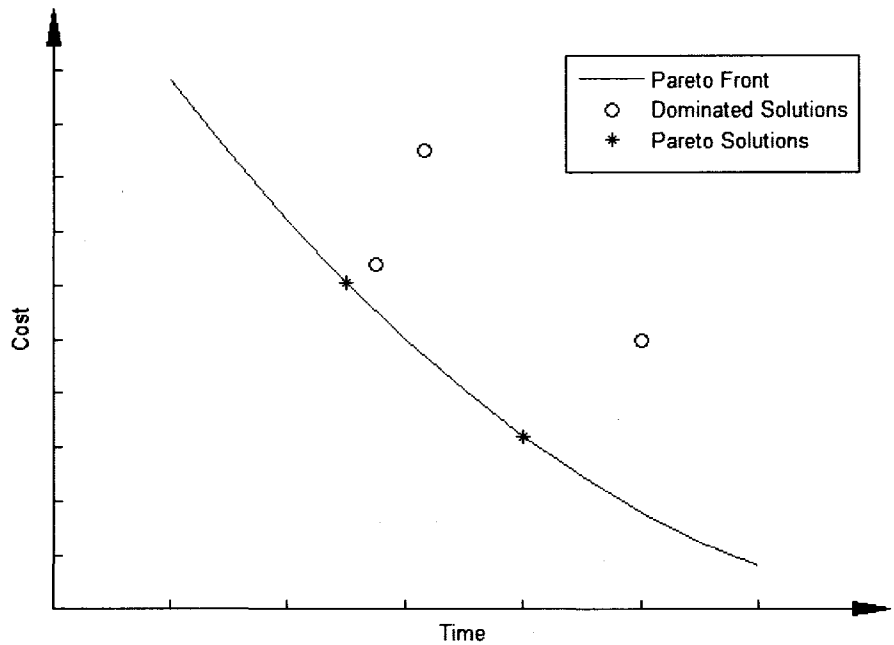

Figure 5.3: The Pareto Frontier for the Cost-Time Example

5.2 Non-Dominated Sorting Genetic Algorithm-II (NSGAII)

Proposed in 2001 by Deb et al. [29, 30], the NSGAII is a powerful and commonly used MO optimization technique that is well suited to solve highly constrained optimization problems. In fact, it was shown in [29] to produce significantly better approximations to the true Pareto frontier then other popular MO evolutionary strategies such as the *strength-Pareto evolutionary algorithm* (SPEA) [31] and the *Pareto-archived evolutionary strategy* (PAES) [32].

Before discussing the foundations of the NSGAII, it is useful to outline the two goals of the algorithm as they dictate the construction of its operators. The first goal is obvious: to identify as many optimal solutions contained within the Pareto frontier as possible. The second goal is to ensure that the solutions obtained by the algorithm are diverse and well spread out over the Pareto frontier.

In order to illustrate the importance of solution diversity, consider two distinct Pareto solution sets used to represent the same Pareto frontier for a bi-objective problem as shown in figure 5.4 [13]. In this figure solution sets (a) and (b) are both non-dominated; however the sets have a varying degree of diversity. Clearly, the solution set with low diversity (a) only outlines a small segment of the Pareto front while the high diversity set (b) gives a good approximation of the same Pareto front as the solutions are well spread out. Thus, solution sets with high diversity give a much better picture of the natural objective function trade-offs.

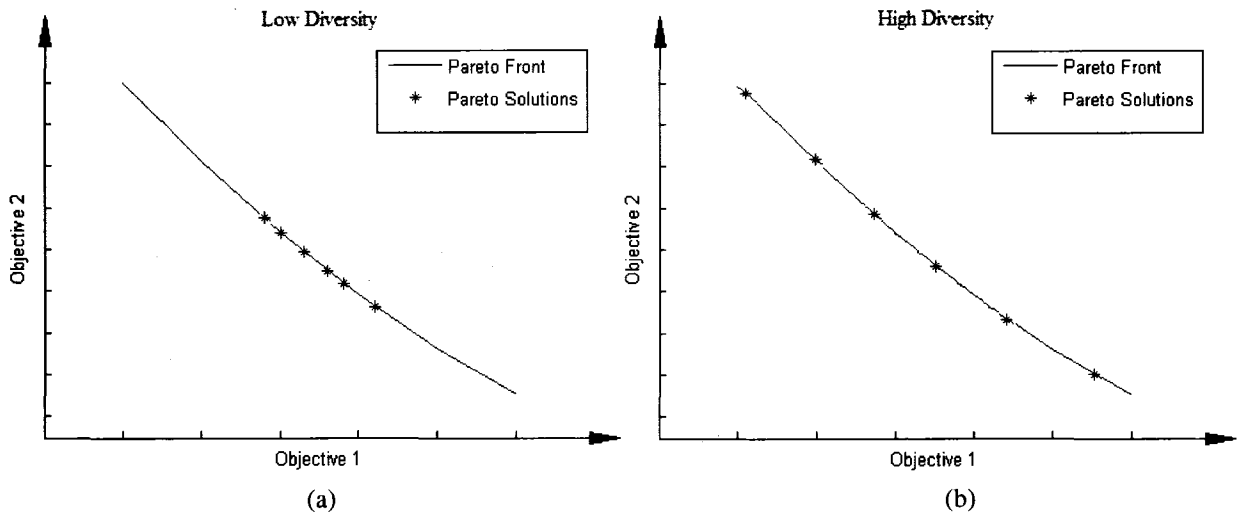

Figure 5.4: Two Pareto Optimal Sets with Distinct Diversity.

At its heart, the NSGAII uses the principles of evolution to evolve a Pareto-optimal set in much the same way the simple genetic algorithm does as was described in chapter 4. However, the definition of chromosome fitness and tournament selection must be tailored to the concepts of non-domination and population diversity to allow the NSGAII to meet the two goals mentioned above. Also, in order to properly implement an elitist strategy to help optimization convergence, the NSGAII main evolution loop must be altered from the single objective GA.

The following sections are used to give an overview of key concepts used by the NSGAII. In section 5.2.1 a description of chromosome fitness and tournament selection for the NSGAII is given. Section 5.2.2 will present an overview of how the NSGAII is constructed.

5.2.1 NSGAII Chromosome Fitness and Tournament Selection

Chromosomes (solutions) used in the NSGAII require more then just an evaluation of the fitness function for each chromosome as is the case with the single objective GAs. While it is still important to evaluate the problem's objective functions, the NSGAII requires three distinct metrics to determine the fitness of each chromosome for parent selection. These metrics are based on the concepts of feasibility, non-domination and diversity. As will be shown in this section, these metrics are vital for the tournament selection operator and the overall ability of the NSGAII to obtain diverse Pareto-optimal solutions.

For any constrained optimization problem, each solution within a population is either feasible or infeasible. If a solution is found to be infeasible, an infeasibility calculation must be performed. The infeasibility calculation is accomplished by determining the normalized value for each solution's constraint violations and summing the absolute values of the violations together [30]. For example, if a solution has the constraint violations $20 < 10$ and $1 > 3$, they are normalized as (20/10-1) and (1/3-1) respectively. After summing together the absolute values of the normalized violations, the infeasibility metric for this arbitrary solution would be 1.667.

The second metric is used to score each solution based on dominance. The NSGAII scoring procedure works in an iterative fashion, by first identifying all non-dominated solutions contained in the population. Non-dominated solutions are all assigned a rank of 1 and constitute the first Pareto front. With these solutions removed

from consideration, the procedure then identifies the resulting non-dominated solutions and assigns them all a rank of 2. This iterative procedure continues until the entire population is assigned a rank based on which front they occupy. It should be noted that the NSGAII considers the ranking of feasible solutions first. When all feasible solutions have been ranked, the NSGAII will the finish the ranking procedure by scoring infeasible solutions based on the infeasibility calculation described above.

An illustration for the ranking of 10 particular solutions of an arbitrary minimization bi-objective problem is shown in figure 5.5. All solutions are assumed to be feasible except for the solution represented by the triangle. It is evident that the NSGAII will obtain 4 distinct sets of rankings. The three rank one chromosomes are globally non-dominated by the population. With rank 1 solutions removed from consideration, the rank 2 solutions are non-dominated by any of the remaining solutions. Similarly, three solutions are identified to occupy the third front. Finally, the infeasible chromosome is given a rank of 4, despite appearing to dominate one of the rank 3 chromosomes.

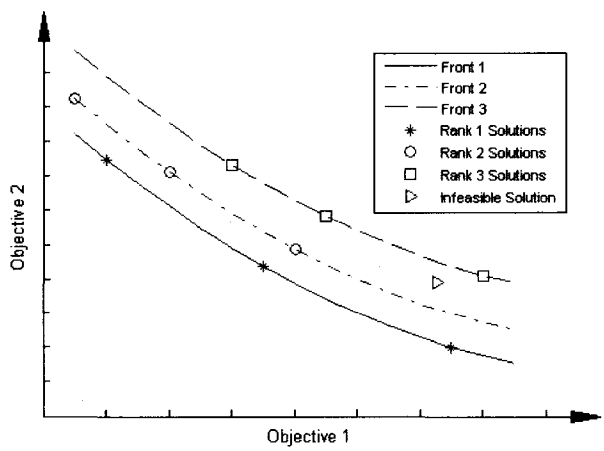

Figure 5.5: Ranking of 10 Chromosomes

The third metric, called the *crowding distance*, is used to estimate the density of solutions surrounding a particular solution for each non-dominated set. The crowding distance allows the NSGAII to understand how diversified each chromosome in the population is.

For each member of a non-dominated set, the crowding distance is obtained by first forming a perimeter around a particular member using the neighbors nearest to it of the same non-dominated set. An example of this perimeter for a member, x_3, is shown in figure 5.6 for a bi-objective problem. The sides of the perimeter are obtained by finding the distances between x_2 and x_4 along each of the objective axis. In order to ensure that these distances are of the same scale, they are normalized by dividing them by the difference between the maximum and minimum values of the corresponding objective functions. Finally, these normalized distances are added together to represent the chromosomes diversity.

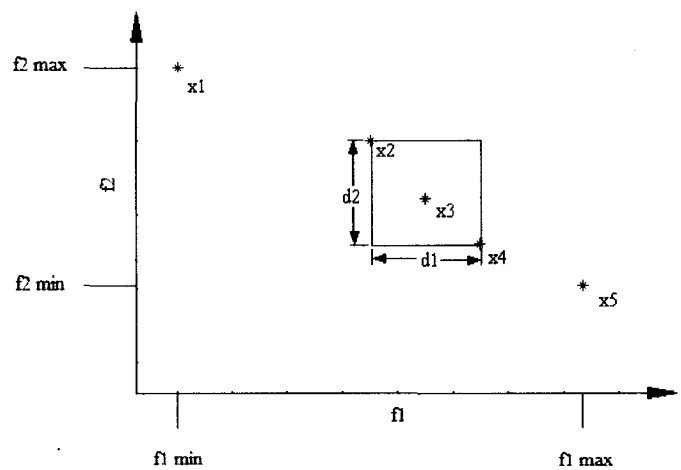

Figure 5.6: Perimeter Created by Nearest Chromosomes of x_3

It should be noted that for boundary members such as x_1 and x_5, the perimeter method does not apply. Instead, a large number is appended to their crowding distance metric to ensure that the NSGAII recognizes that they are the end points of their non-dominated front.

The importance of the three metrics is evident when the possible scenarios of tournament selection are considered as they define the outcome. Since the tournament selection operator is usually coded to randomly select two chromosomes at a time, there are four scenarios that can occur. The scenarios and their outcomes are listed as follows:

1. Both chromosomes are of the same non-dominated set. The winner of this tournament is the chromosome that has the largest crowding distance.
2. Both chromosomes are feasible but are part of different non-dominated sets. The tournament winner is the chromosome with the lowest rank.
3. One chromosome is feasible while the other is not. The feasible solution is always chosen to be the winner.
4. Both chromosomes are infeasible. The chromosome that has the lowest infeasibility value is the winner of the tournament.

From the list it is evident that the infeasibility, non-domination and diversity metrics allows the NSGAII to always pick the best chromosome for each tournament scenario. For instance, if two solutions are of the same rank, it is best to select the chromosome with the higher crowding distance in order to "fill in" portions of the Pareto frontier that are missing. Picking the right solution to be added to the parent pool helps to find feasible solutions that are near Pareto-optimal with a high level of diversity.

5.2.2 NSGAII Main Loop Strategy

Before entering the main evolution loop, the NSGAII operates in a similar fashion as the single objective genetic algorithm. In the first generation of artificial evolution, the NSGAII starts by creating a randomized population, P_1 of size N where it then assigns fitness to each member based on the three metrics described in section 5.2.1. Next, tournaments selection is performed to pick a pool of parents of size N. Finally, the usual genetic recombination and mutation operators are invoked to create a child population, Q_1 of size N.

The subsequent iterations are different from the initial generation. This is due to the fact that in order to retain the best chromosomes from generation to generation (elitism), the child population must be compared with the parent population. From this comparison, the best overall N chromosomes are selected from the two populations based on non-domination and crowding.

The process of the ith iteration is shown in figure 5.7. At the beginning of the iteration the parent population, P_i, and the child population, Q_i, are merged into one large population, R_i, of size 2N. Each chromosome in R_i is then placed into its respective non-dominated set using non-dominated sorting. This forms multiple Pareto fronts. Chromosomes contained within the first front, F_1, are the best overall chromosomes and should be preserved into the subsequent parent population, P_{i+1}, to ensure elitism. If the size of F_1 is smaller than P_{i+1}'s size N restriction, each chromosome contained in the front is assigned a crowding distance and passed on to the P_{i+1} population. The additional

members of P_{i+1} are obtained from the remaining fronts in the ranked order. Thus, the next group of chromosomes to be placed into P_{i+1} is from the second non-dominated front, followed by the third and so on. This process continues until it reaches a front that cannot be completely accommodated by P_{i+1}'s size N restriction. When it reaches this front, call it F_n, each chromosome must be ranked according to its crowding distance, where larger crowding distance means better rank. The best ranked chromosomes from F_n are then placed into P_{i+1} one at a time until the overall size of P_{i+1} contains N chromosomes. All chromosomes that have not been placed into P_{i+1} are discarded from future consideration. With the elite parent population formed the evolutionary operators (tournament selection, parent recombination and mutation) are invoked to create the next generation child population Q_{i+1}. This ends one iteration of the NSGAII's main evolution loop.

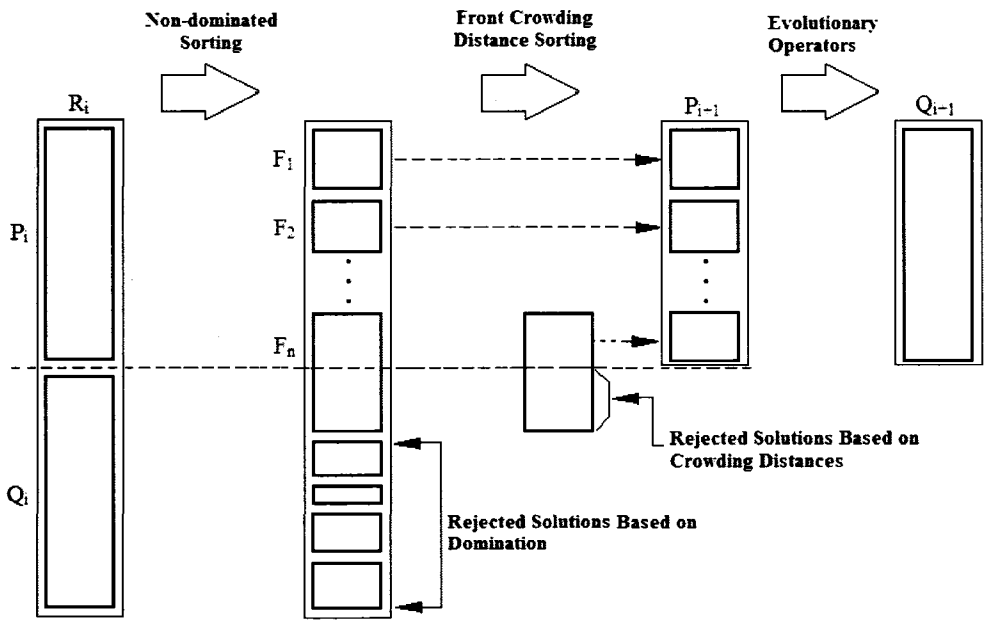

Figure 5.7: NSGAII Main Loop Strategy [29]

5.3 An Illustration of NSGAII Optimization

The purpose of this section is to apply the NSGAII to a simple MO optimization problem to show its effectiveness for obtaining Pareto-optimal solutions. In section 5.3.1, a description of the optimization problem is given along with a description of its optimal solution. Section 5.3.2 will present the optimal results obtained by the NSGAII.

5.3.1 Problem Overview

Consider the following simple bi-objective optimization problem [13]:

Minimize $f_i(x), i \in \{1,2\}$ (5.1)

Subject to:

$$-10 \leq x \leq 10 \tag{5.2}$$

where

$$f_1(x) = x^2 \tag{5.3}$$

$$f_2(x) = (x-2)^2 \tag{5.4}$$

Figure 5.8 shows the plots for the optimization problem's objective functions for values of x between -4 and 4. The minimum solution for objective functions f_1 and f_2 are

located at 0 and 2 respectively. Clearly, there is not a value of x that minimizes both objective functions simultaneously.

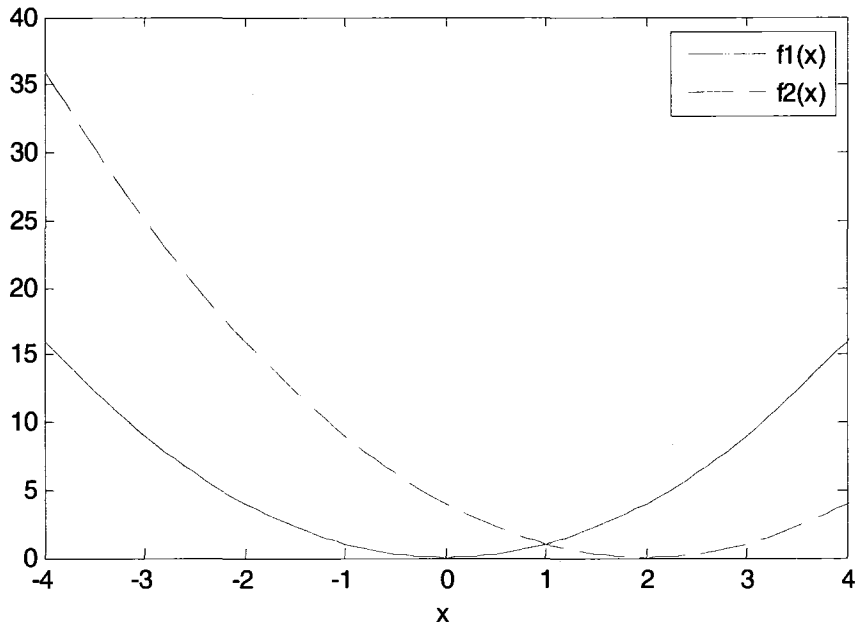

Figure 5.8: Plot for Objective Functions, f_1 and f_2

Turning our attention to Pareto-optimality, it is obvious that there is an objective function trade-off region for $x \in [0, 2]$ as function f_1 increases while f_2 decreases over this range. Solutions contained in the sets $x \in [-10, 0)$ and $x \in (2, 10]$ are dominated by at least one solution in the trade-off range. Thus, the expected Pareto-optimal solution should consist only of the region defined by the set $x \in [0, 2]$.

While figure 5.8 indirectly shows the Pareto solutions, a better illustration of the Pareto frontier can be obtained by plotting the objective space for the optimization problem. Figure 5.9 shows the plot of the $f_1(x)$ versus $f_2(x)$ as x is varied from -3 to 3. It is evident from this figure that the Pareto frontier is given by the sets $f_1 \in [0, 4]$ and

$f_2 \in [0, 4]$ which is shown in the figure as a solid line. Note that these ranges correspond to the set $x \in [0, 2]$. The dominated sets are represented by the dashed lines are obtained from the sets $x \in [-10, 0)$ and $x \in (2, 10]$.

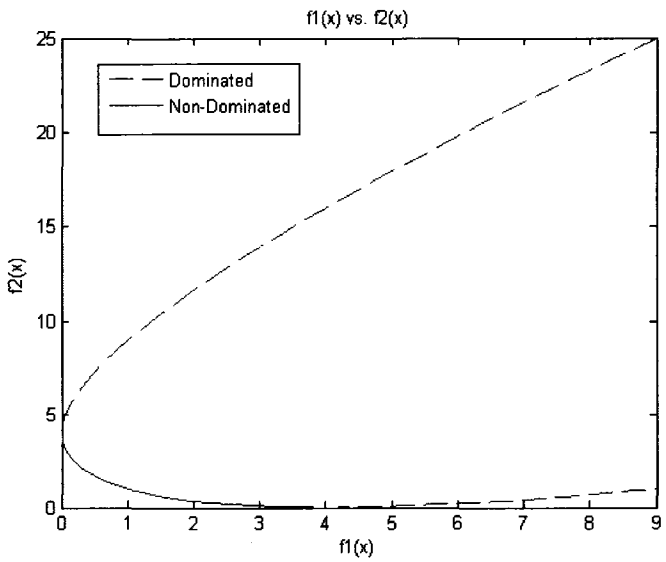

Figure 5.9: Illustration of Pareto Frontier

5.3.2 Results of NSGAII Optimization

The optimization results presented here were obtained by using MATLAB 7.0 to code the NSGAII algorithm. The following table shows important NSGAII parameters used for this application. Equation 4.4 was used to decode the binary strings into a continuous decimal representation. It should be noted that unlike the GA single objective optimization problem found in section 4.3, even a simple MOP requires a significant number of chromosomes to approximate the Pareto frontier.

Table 5.1: NSGAII Settings for Optimization Problem

X Variable bits	10
Population Size	100
Generation Number	150
Mutation Probability	0.001
Crossover Probability	0.85

Figure 5.10 shows the objective space of optimization problem for an initialized random population generated by the NSGAII. It is clear from this figure that the population is well spread out over the objective space which will allow the NSGAII seek out promising areas. It is also evident that the population consists mostly of dominated solutions while only 10 solutions are contained within the Pareto front.

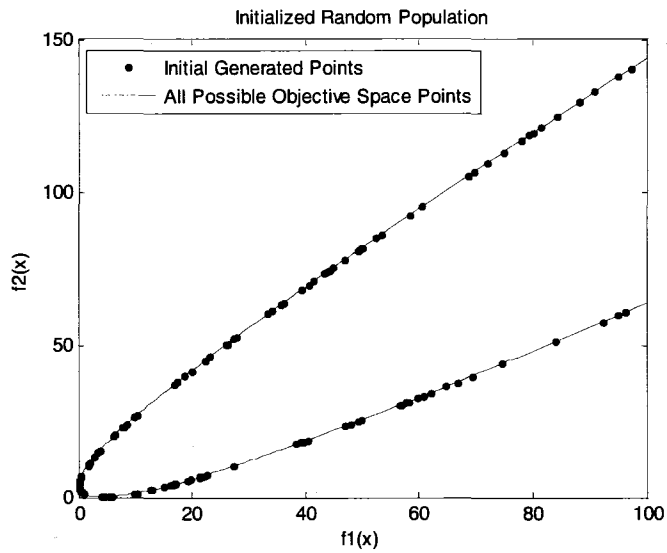

Figure 5.10: Objective Space for the Initial Random Population

With the initial population created, the NSGAII enters the evolution loop for 150 generations. The resulting solution obtained by the NSGAII after these generations is presented in figure 5.11. As expected, the final population contains only non-dominated solutions. Further, by superimposing the true Pareto front onto the NSGAII solution plot, it is apparent that the solutions are Pareto-optimal. This conclusion was also verified by ensuring that each Pareto solution control variable (x) setting was between 0 and 2.

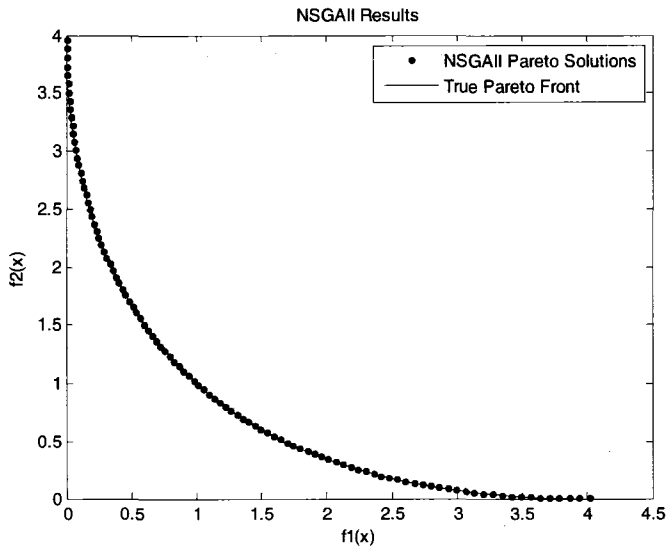

Figure 5.11: Final Population

Another excellent result obtained here is that the Pareto solutions are very well distributed over the entire Pareto front without any significant gaps between solutions. This spread shows the effectiveness of the NSGAII's crowding operator ability to add value for obtaining a better approximation of the true Pareto front.

5.4 Summary

This chapter provided a fundamental overview of MO optimization problems. From the discussion, it is obvious that it is impossible to obtain a single optimal solution to optimize all objectives in question. However, using the concepts of Pareto-optimality, it is possible to define a set of solutions that describe the optimal trade-offs between competing objectives. As all of these solutions are in a sense optimal, it is beneficial to have as many of them as possible so the best solution from the set can be selected based on other criteria.

Evolutionary techniques have been widely applied to MOPs because of their global searching capability and the ability to obtain multiple Pareto-optimal solutions in one run. One of the most popular MO evolutionary programming strategies, the NSGAII, was overviewed in this chapter. Using the fundamentals of evolution, non-domination and solution diversity, the NSGAII has the ability to obtain multiple Pareto-optimal solutions in one run of the algorithm that are well spread out over the Pareto frontier. This was clearly shown through a bi-objective optimization problem presented in this chapter.

The next chapter will focus on applying the NSGAII to two reactive power planning case studies. This will put the tool to the test as it is exceedingly more challenging than the optimization problem presented in this chapter.

Chapter 6

Application of the NSGAII to Reactive Power Planning

6.0 Introduction

Chapter 3 introduced a challenging power systems optimization problem known as the multiple objective reactive power planning problem (RPP). In all of its various formulations, the RPP was shown to be difficult to optimize for traditional optimization techniques. It was shown in chapter 4 that genetic algorithms have the inherent ability to seek out global or near global optimal solutions to difficult optimization problems. This was demonstrated by applying it to a single objective nonlinear optimization problem and the optimal power flow (OPF). However, the foundations of the single objective GA cannot treat multiple objectives independently. A powerful technique known as the *non-dominated sorting genetic algorithm-II* (NSGAII) was introduced in chapter 5 that extends the capability of genetic algorithms to handle multiple objectives independently

using the concepts of Pareto-optimality. The ability of the NSGAII to solve the RPP has yet to be demonstrated.

The aim of this chapter is to evaluate the effectiveness of the NSGAII for solving RPPs that contain two objective functions as described below. Two case studies were performed using two distinct power systems. For both case studies, the NSGAII was required to generate a feasible and non-dominated set of shunt compensation schemes that correct for system operation constraint violations due to large system load increase.

This chapter is organized as follows: Section 6.1 will give an overview of the common assumptions made for both studies and the simulation test environment. In section 6.2, a RPP case study using a 6-bus power system [21] will be discussed, where the optimization objectives were to minimize the costs of shunt reactive power allocations and active power transmission losses. Section 6.3 will provide a RPP case study using a modified IEEE 30-bus power system [28], where the goals of optimization were to minimize shunt reactive power allocations costs and average load bus voltage deviation. Section 6.4 will summarize the chapter.

6.1 Case Study Assumptions and Testing Environment

For the purposes of the two case studies presented in this chapter, the following important assumptions will be made with respect to RPP:

- Reactive compensation will be considered for the systems operating only at peak load. The peak load will be based on a forecasted load growth that increases apparent power demand at all system load bus locations *uniformly*. This loading will place significant stress on the systems and will violate multiple operational constraints.
- Possible reactive shunt installation locations are predetermined. No reactive compensation will be applied to any location outside of the specified sites. This is a practical consideration as many power systems cannot install shunt compensation at every location in the system.
- A predefined active power generation schedule will be given and will be held constant throughout the optimization procedure. The only variability to the total generator active power output is from the system's reference bus.
- Potential compensation schemes will not be influenced by the effects of various contingencies, such as line outages.
- VAr sources (Q_c) will be available in discrete banks only. Each bank will be rated to inject 0.5 MVAr of reactive power into the system at nominal voltage. The nominal voltage of 1.0 p.u will be assumed.
- The fixed installation cost for reactive compensation devices is assumed to be $50,000 at each site chosen for compensation. The purchasing costs for the devices will be $10,000 per MVAr.

In order to perform the studies, NSGAII based RPPs were coded in MATLAB 7.0. MATLAB was chosen as the test setup as an interface between it and a MATLAB based power systems analysis toolbox called MATPOWER [28]. Moreover, MATPOWER is fully capable of solving the required power flows for determining constraint violations which removed the need to develop a power flow software package. The test PC was laptop containing a Pentium IV 3.0GHz processor and 512MB of RAM.

6.2 6-Bus Case Study

In this section, a RPP case study was performed where the goal of optimization was to minimize both the costs of reactive power compensation devices and the active power transmission losses for a large load forecast. These objectives were discussed in detail in chapter 3. The RPP presented here uses the same objectives as the RPP performed by Lai [3], except the objective functions will be treated independently instead of augmenting the objectives together.

The 6-bus power system used for this study is shown in figure 6.1 [21]. The system consists of 3 generators, 3 loads and 11 transmission lines. Note that bus 1 is the reference bus. All system parameters along with the initial load demand and generation schedule are available in Appendix B using an apparent power base of 100 MVA. Table 6.1 lists important operational constraints assumed for this case study.

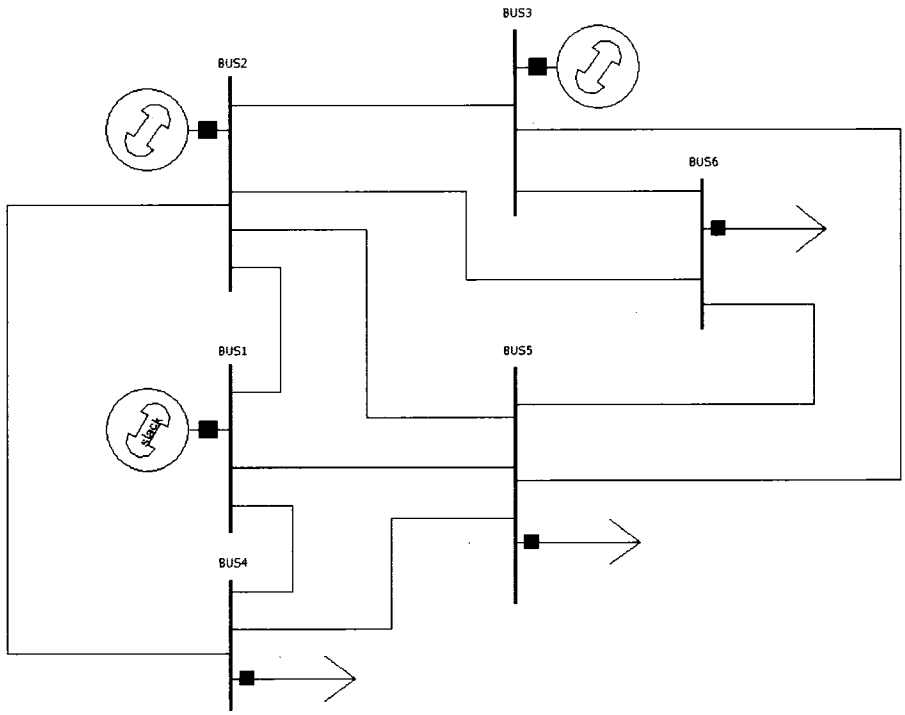

Figure 6.1: Single Line Diagram of the 6-Bus Test System [21]

Table 6.1: Operational Constraints for the 6-bus Power System

Generator Reactive Power Limits (MVAr)			
Bus	1	2	3
Q_g^{max}	100	100	100
Q_g^{min}	-10	-10	-10
Generator Active Power Limits (MW)			
Bus	1	2	3
P_g^{max}	165	165	165
P_g^{min}	0	30	40
Load Bus Voltage Limits (p.u)			
V_{bus}^{max}		V_{bus}^{min}	
1.05		0.95	
Generator Voltage Limits (p.u)			
V_g^{max}		V_g^{min}	
1.05		0.95	
Transmission Line Apparent Power Limits (MVA)			
$S_{trans} \leq 130$			

In the following sections, details about the specifications of the case study and NSGAII will be given. Along with this, a discussion on the results obtained by the NSGAII will be provided.

6.2.1 Load Forecast and Generation Schedule

The initial load demand and generation schedule do not violate any operational constraints. In order to emulate load growth that facilitates operational constraint violations, active and reactive power demand by each load was increased to 150 MW and 120 MVAr respectively. Thus, the total active power and reactive power demand was 450 MW and 360 MVAr.

The total active power generation capacity for the power system was 495 MW. Taking into account that the load demand nearly meets the total generation capacity and the active power limits of the generators, the active power of generators 2 and 3 were set to their upper limits of 165 MW. As the reference generator must make up for any active power generation deficiency and provide the active power for transmission losses, the specified generation schedule ensures that the reference generator does not violate its own active power constraint.

6.2.2 6-Bus Base Case Power Flow

Before beginning with the planning of a reactive power compensation scheme, it is important to first verify that the system cannot be operated with the increased load demand. A base case power flow was performed to get an idea of the severity of the constraint violations. For the base case power flow, the generator voltage levels were set to 1p.u. Table 6.2 lists all the constraint violations. It should be noted that even after increasing the generator terminal voltages to their maximum levels, the operational constraint violations from table 6.2 were still apparent.

Table 6.2: Operational Constraint Violations for the 6-Bus System

Bus	3	4	5
V_{bus} (p.u)	0.853	0.819	0.866
Bus	2	3	-
Q_g (MVAr)	206.68	159.19	-
Line	2-4	3-6	-
S_{trans} (MVA)	140.26	158.60	-

It is evident from table 2 that five of the operation constraints are being violated by large margins. As was discussed in chapter 2, remote reactive power transmission can lead to low voltages and congested transmission lines as are seen in the above table. These results show the real need to add local VAr support to the system in order allow the system to operate within desired specifications.

6.2.3 6-Bus Case Study Control Parameters and NSGAII Specifications

This case study used six control parameters for the RPP: three generator bus voltages (V_g) and three VAr source allocation busses (Q_c). The VAr allocation buses were chosen on the basis that each of the system's loads demand significant amounts of reactive power that can be met with local reactive power support.

Table 6.3 gives the NSGAII parameters used for this case study. For the purposes of this test case, each generator voltage was coded using the same number of bits. Similarly, each reactive source allocation was coded using the same number of bits.

Table 6.3: NSGAII Parameters for the 6-Bus Case Study

Population Size	100
Generations	150
Mutation Probability	0.001
Recombination Probability	0.85
V_g Variable Bits	6
Q_c Variable Bits	9

As this case study has both continuous and discrete control parameters, two methods of control variable decoding must be invoked. For the voltage control parameters, the conversion of each binary string into a continuous decimal value was done using equation 4.4.

In order to properly account for the discrete step size of the reactive source allocations, the following equation was used to decode a binary VAr source allocation i, into a decimal number:

$$Q_{ci} = dec(str_{ci}) * 0.5 * 1 \text{ MVAr} \quad (6.1)$$

where $dec(str_{ci})$ is conversion of the binary encoded VAr source parameter, i, to its base 10 representation. As 9 bits are used to represent each VAr source, equation 6.1 decodes each binary VAr source string in discrete steps of 0.5 MVAr over a range from 0 to 255.5MVAr. This range is more than sufficient to meet load reactive power demand as each load only demands 120 MVAr.

6.2.4 6-Bus Case Study Results

As the NSGAII is a heuristic optimization technique, it is not guaranteed to converge on the identical solution with each run of the algorithm. With this knowledge, multiple runs were performed in order to observe the ability of the NSGAII to locate non-dominated frontiers. Figure 6.2 shows the results of two of these runs. From this figure it is clear that the NSGAII managed to obtain similar solution sets.

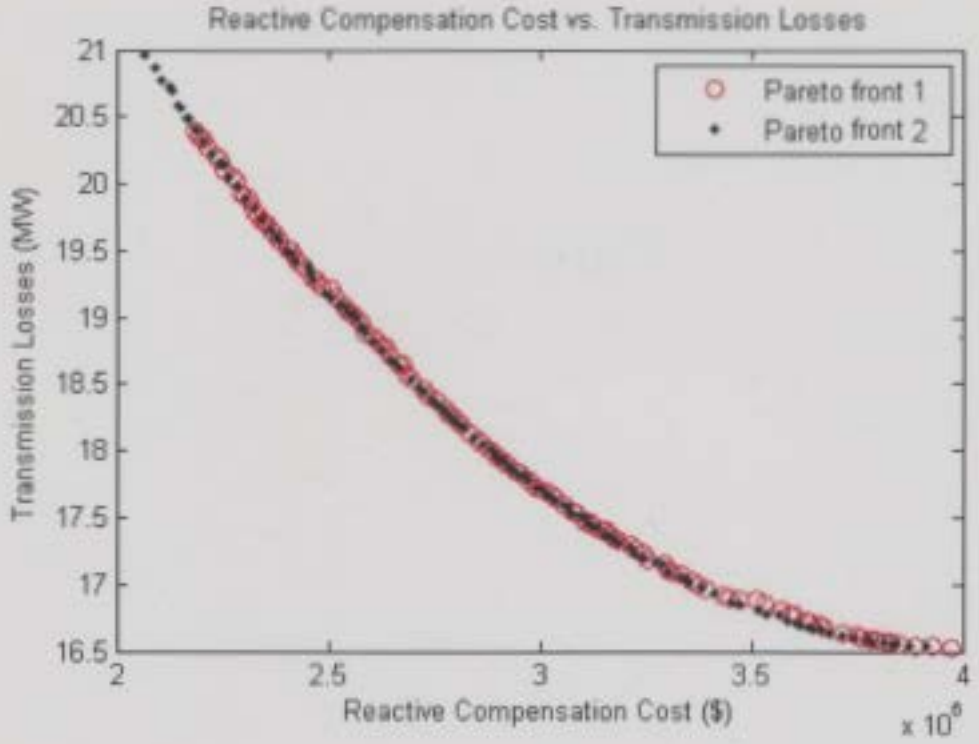

Figure 6.2: Two Pareto Fronts for the 6-Bus Case Study

Regardless of the slight discrepancies between the two solution sets, it is observed that the NSGAII located only non-dominated solutions for each set. Each of the solutions contained in the frontiers are feasible as no operation constraint was found to be violated. Also, due to the large population used in this case study, both solution sets are well distributed over the Pareto-front and contain no significant gaps over their respective frontier. These are two excellent results of the NSGAII RPP case study.

The NSGAII obtained non-dominated solutions for this case study due to the fact that minimization of VAr source allocations costs and transmission line losses are in direct conflict with each other. Clearly from figure 6.1, with more money spent on VAr

sources, lower line losses are achieved. This is an intuitive result based on the discussion of reactive power compensation from chapter 2.

The obvious trade off between VAr costs and transmission line losses is best illustrated by considering the maximum and minimum cost solutions for the second Pareto frontier. These solutions' control parameter settings are given in table 6.4. It is apparent from the table that the maximum cost VAr source allocations are significantly higher than the minimum cost VAr sources. As a result of these allocations, it was found that the maximum VAr source scheme induces a $3,915,000 cost while the minimum cost scheme has a cost of $2,065,000. The maximum and minimum cost solutions have transmission line losses of 21MW and 16.5 MW respectively. Thus, by allowing an additional spending of $1,850,000 it is possible to reduce the transmission losses by 22%.

Table 6.4: Control Parameter for Maximum and Minimum Solutions of Pareto Front Two

Control Parameter	Maximum Cost Solution	Minimum Cost Solutions
V_{g1} (p.u)	1.050	1.050
V_{g1} (p.u)	1.050	1.050
V_{g1} (p.u)	1.050	1.050
Q_{c4} (MVAr)	128.0	64.50
Q_{c5} (MVAr)	127.0	79.00
Q_{c6} (MVAr)	121.5	48.00

Ultimately, the choice of the "optimal" solution is up the planner. There may be many reasons for choosing one solution over another. For instance, if the cost of equipment is of great concern and losses are of secondary importance, the minimal cost

solution should be chosen. It is an acceptable solution as the power system equipped with the minimum VAr source scheme can handle the load forecast without violating operational constraints. If transmission losses are of primary concern, the 22% reduction in line losses between the maximum and minimum cost solutions may be very attractive and should be favored. This is especially true if the system is known to operate at peak loading for long periods of time and the costs of MW losses per hour is high. If however, the VAr source costs and MW losses are of the same importance, the best solution would be contained somewhere in the middle of the Pareto-front as neither objective is minimized but a better balance between the two objectives is realized.

As a further example of how external information not given in the problem's definition may bias the choice of an optimal solution, consider again the control parameter settings in table 6.4. The load bus voltages for this power system under these control parameter settings are shown in table 6.5. It is apparent from this table that the minimal cost solution is close to bordering on the bus voltage limits. Thus, this solution is the minimal feasible solution obtained by the NSGAII. However, the maximum cost bus voltages are much closer to their nominal value of 1.p.u. With regards to voltage stability and the safety of power system equipment, the voltages pertaining to the maximum cost solution are significantly more attractive than the minimum cost solution.

Table 6.5: 6-Bus System Load Voltages for Maximum and Minimum Cost Solutions

Control Parameter	Maximum Cost Solution	Minimum Cost Solutions
V_{bus4} (p.u)	1.015	0.963
V_{bus5} (p.u)	1.012	0.954
V_{6bus6} (p.u)	1.023	0.966

6.3 IEEE 30-Bus Case Study

In this section, a RPP case study was performed where the goal of optimization was to minimize the costs of VAr source compensation devices and the average load bus voltage deviation [33]. The costs objective is identical to the cost objective used for the 6-bus case study. The average load bus voltage deviation was discussed in chapter 3. The creation of a single objective by weighting and summing these two objectives would be difficult as it would be difficult to convert voltage profile into a dollar value. Thus, these objectives should be treated independently.

The IEEE 30-bus power system used for this study is shown in figure 6.3 [28]. The system consists of 6 generators, 21 loads and 41 transmission lines. Note that the bus 1 is the reference bus. All system parameters along with the initial load demand and generation schedule are available in Appendix C using an apparent power base of 100 MVA. Table 6.6 lists important operational constraints assumed for this case study.

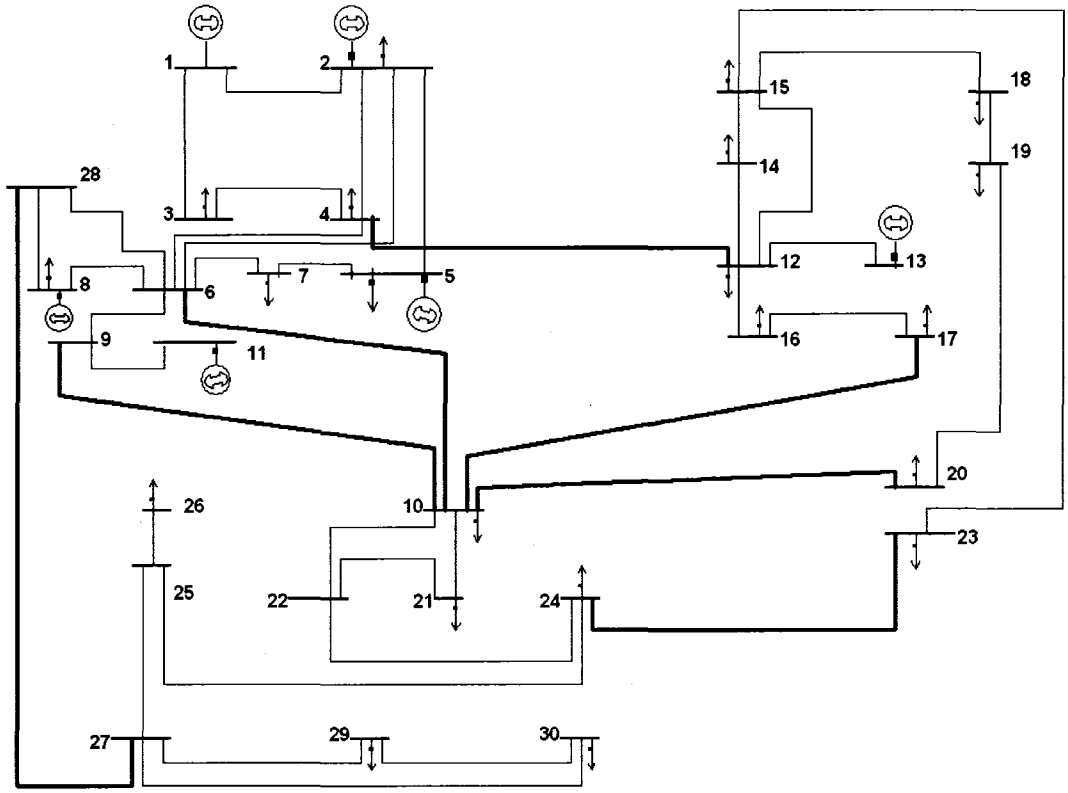

Figure 6.3: One Line Diagram of the IEEE-30 Test System [28]

Table 6.6: Operational Constraints for the 30-bus Power System

Generator Reactive Power Limits (MVAr)						
Bus	1	2	5	8	11	13
Q_g^{max}	150	60	62.5	48.7	40	44.7
Q_g^{min}	-20	-20	-15	-15	-10	-15
Generator Active Power Limits (MW)						
Bus	1	2	5	8	11	13
P_g^{max}	100	140	100	100	100	100
P_g^{min}	0	0	0	0	0	0
Load Bus Voltage Limits (p.u)						
V_{bus}^{max}				V_{bus}^{min}		
1.05				0.95		
Generator Voltage Limits (p.u)						
V_g^{max} (p.u)				V_g^{min} (p.u)		
1.05				0.95		
Transmission Line Apparent Power Limits (MVA)						
$S_{trans} \leq 110$						

In the following sections, details about the specifications of the case study and NSGAII will be given. Along with this, a discussion on the results obtained by the NSGAII will be provided.

6.3.1 Load Forecast and Generation Schedule

For the purposes of this test case the initial real and reactive power demand of each system load bus was multiplied by 2 in order to uniformly emulate a future load growth. Thus, the total real and reactive power demanded by the system was 566.8 MW and 252.4 MVAr respectively.

The active power generation schedule used in this case study is shown in table 6.7. Similarly to the 6-bus case study, all generators except for the reference generator were set to their maximum active power output limit. As the total generation capability for the system was 640 MW, the specified schedule helps to ensure that the reference generator does not exceed its active power output by having to make up for deficiencies in power generation.

Table 6.7: Generation Schedule for the 30-Bus Case Study

Generator Active Power Schedule					
Bus	2	5	8	11	13
P_g (MW)	140	100	100	100	100

6.3.2 30-Bus Base Case Power Flow

The base case power flow presented here was performed to get an idea of the severity of the operational constraint violations. For the base case power flow, all generator bus voltages were maintained at 1 p.u.

Table 6.8 lists all the violations that occur due to the forecasted load increase. Due to the forecasted load demand a significant portion of the system's constraints are being violated. Many of the load bus voltages are well below the specified 0.95 p.u value while half of generators are operating well above their maximum reactive power limits. These results show that the addition of reactive power support to the system will help the power system operate safely under peak loading.

Table 6.8: 30-Bus Constraint Violations for the Base Case Power Flow

Bus	**9**	**10**	**12**	**14**	**15**	**16**	**17**	**18**	**19**	**20**
V_i (p.u)	0.941	0.908	0.944	0.908	0.894	0.910	0.897	0.870	0.863	0.872
Bus	**21**	**22**	**23**	**24**	**25**	**26**	**27**	**29**	**30**	-
V_i (p.u)	0.878	0.880	0.866	0.848	0.852	0.809	0.878	0.826	0.799	-
Bus	**5**	**8**	**13**	-	-	-	-	-	-	-
Q_{gi} (MVAr)	90.38	106.32	47.43	-	-	-	-	-	-	-

6.3.3 30-Bus Control Parameters and NSGAII Specifications

The total number of control parameters used in this case study was ten. This case study limited the possible VAr source allocations to four different buses. These buses

were selected based on areas of large reactive power demand and reactive power transmission. As VAr compensation will have a strong local impact on bus voltages near the VAr allocation sites, it was important to distance the sources throughout the network in order to help raise the voltages of all system buses. For this case study the buses that were selected for compensation are 5, 17, 18, and 27. Also, the six generator terminal voltages were used as control variables in this case study.

Table 6.9 gives the NSGAII parameters used for this case study. Note that an increased population size was used over the case study in section 6.2 as this case study is of larger scale and has many more operational constraints. The increased population helps to ensure that a more rigorous exploration of the search space is performed by NSGAII. The larger population used in this case study is at the expense of longer processing times.

Table 6.9: NSGAII Parameters for the 30-Bus Case Study

Population size	150
Number of generations	150
Mutation probability	0.001
Crossover probability	0.85
V_g parameter bits	6
Q_c parameter bits	7

For the purposes of this test case, each generator voltage was coded using the same number of bits. The decoding of the voltage control binary strings is done using equation 4.4. Each VAr source was also coded using the same number of bits. Equation

6.1 was used to decode each VAr source binary string into a decimal value. Thus, each VAr source control variable was in discrete steps of 0.5 MVAr over the range 0 MVAr to 63.5 MVAr

6.3.4 IEEE 30-Bus Case Study Results

As with the 6-bus case study, multiple runs of the NSGAII for solving the 30-bus RPP were done to observe the variability in the obtained solutions. Presented in figure 6.4 are the three non-dominated solutions sets obtained for three separate runs of the NSGAII. All solutions contained within these Pareto fronts do not violate any operating constraints.

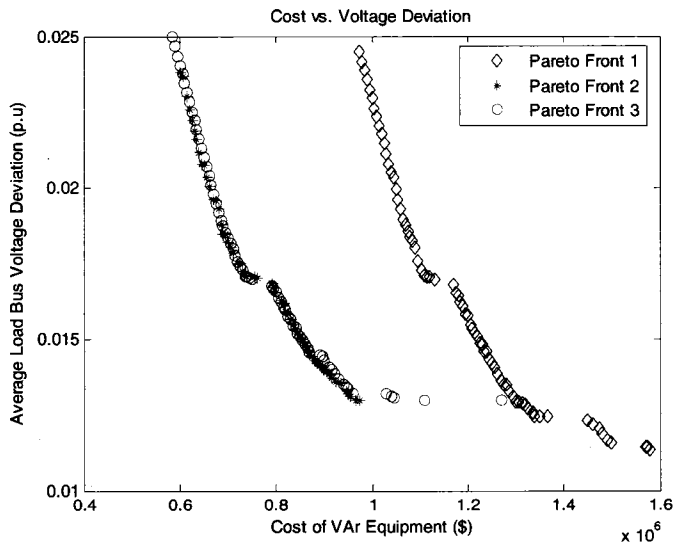

Figure 6.4: Pareto Frontiers for the 30-Bus Case Study

It is apparent from the figure that the NSGA-II managed to converge on two distinctive non-dominated fronts. While fronts two and three have similar solution sets, front one is significantly different. The primary reason for this variable convergence is fact that there are well over $1.8*10^{19}$ distinct control parameter configuration possibilities while the NSGA-II only uses 30000 power flows in the attempt to locate the true Pareto frontier! It is clear however, that in the case of each of the fronts shown in the figure, the solution sets are all non-dominated and well distributed over their established front.

In figure 6.4, front one's non-dominated solutions induce significantly larger costs to obtain a similar load bus voltage deviation than the second and third frontiers, hence is called a *local* optimal solution. For instance, in the case of minimal VAr source cost solutions for fronts one and two, the parameter configurations found in table 6.10 were obtained. Clearly the cost of front one's minimum cost solution far exceeds the cost of front two's solution while giving a similar load bus voltage profile. With this train of thought, it is apparent that the majority of solutions contained within front one are dominated by both front two and three solutions.

Table 6.10: Example Solutions Taken from Two Pareto Frontiers

Front	V_{g1}	V_{g2}	V_{g5}	V_{g8}	V_{g11}	V_{g13}	Q_{c5}	Q_{c17}	Q_{c18}	Q_{c27}	Cost	V_{dev}
1	1.05	1.05	1.02	1.01	1.05	1.05	32	0	18	32.5	9.75e+005	0.024487
2	1.05	1.05	1.01	1.02	1.05	1.05	0	0	16	32.5	5.85e+005	0.024979

The trend obtained by the NSGAII for reactive power planning is as expected. In each of the fronts we see that as we devote more money to installing reactive

compensation in the network, the load bus voltage profile reduces significantly. To illustrate this fact, consider the maximum and minimum cost solutions of front two, where the costs of these solutions are $585,000 and $1,270,000. Their reactive power allocation is shown in table 6.11.

Table 6.11: Maximum and Minimum VAr Allocations for Pareto Front Two

	Minimum Cost Allocations	**Maximum Cost Allocations**
Q_5 (MVAr)	0.00	22.50
Q_{17} (MVAr)	0.00	20.00
Q_{18} (MVAr)	16.00	31.00
Q_{27} (MVAr)	32.50	33.50

The results of the power flows using the minimum and maximum VAr installations are shown in tables 6.12 and 6.13 respectively. From these tables, it is apparent that increasing spending on reactive installations improves the load bus voltage profile. The minimum cost solution has many bus voltages that deviate sharply from the desired 1 p.u voltage. By increasing the spending on reactive sources fewer voltages deviate greatly from the desired 1 p.u voltage. If a planner believes that the average load bus voltage deviation is very important, it may be worth the extra investment costs to implement the maximum cost solution. However, if minimizing the costs of VAr sources is more attractive, the minimal cost solution may be the most attractive as the solution still accommodates the load increase without violating any operational constraints.

Table 6.12: Pareto Frontier 2 Minimal Cost Load Bus Voltage Profile

Bus	**2**	**3**	**4**	**6**	**7**	**10**	**12**	**14**	**15**	**16**
V_i ***(p.u)***	1.029	1.0243	1.018	0.998	1.002	0.983	1.01	0.983	0.976	0.981
Bus	**17**	**18**	**19**	**20**	**21**	**22**	**23**	**24**	**25**	**26**
V_i ***(p.u)***	0.972	0.974	0.96	0.964	0.96	0.962	0.957	0.95	0.992	0.955
Bus	27	28	29	30	-	-	-	-	-	-
V_i ***(p.u)***	1.037	1.017	0.996	0.972	-	-	-	-	-	-

Table 6.13: Pareto Frontier 2 Maximum Cost Load Bus Voltage Profile

Bus	**2**	**3**	**4**	**6**	**7**	**10**	**12**	**14**	**15**	**16**
V_i ***(p.u)***	1.018	1.014	1.006	0.989	1.01	1.006	1.02	1	0.998	1.004
Bus	**17**	**18**	**19**	**20**	**21**	**22**	**23**	**24**	**25**	**26**
V_i ***(p.u)***	1.007	1.02	0.999	0.999	0.983	0.985	0.978	0.97	1.002	0.965
Bus	27	28	29	30	-	-	-	-	-	-
V_i ***(p.u)***	1.041	1.005	1.00	0.976	-	-	-	-	-	-

6.4 Summary

This chapter evaluated the NSGAII's performance for the identification of Pareto optimal solutions for specific multi-objective RPP formulations. Case studies were performed on a 6-bus power system and the IEEE 30-bus test system. From the results it is apparent that the NSGAII obtained feasible non-dominated solution sets that are well spread out over the non-dominated fronts. The results also showed that the NSGAII correctly identified the intuitive trade-off between reactive power support and transmission line losses as well as the trade-off between reactive power support and power system violate profile.

One of the pit-falls of heuristic optimization techniques is also apparent from the results however. The NSGAII managed to identify two significantly different Pareto frontiers for the 30-bus case study. Thus, even after multiple solutions are obtained from the NSGAII it is not quite clear that the obtained results are truly *global* optimal. However, considering that there are no other widely accepted techniques based on traditional mathematics that can handle multi-objectives without a weighting scheme, the evolutionary approach performed well.

Chapter 7

Conclusions and Future Work

In this thesis, the RPP was shown to be an exceedingly difficult optimization problem as its formulation is multi-objective, partially discrete, non-linear, highly constrained and of large scale. As power systems rely on reactive compensation as a means to overcome operational constraint violations due to increased load demand, tool sets that rise above the limitations of classical optimization techniques must be developed in order to allocate compensation in an optimal way.

Heuristic strategies are powerful optimization tools that are known to overcome many of the limitations imposed by classical techniques. This thesis investigated the application of a heuristic technique called the NSGAII to RPPs. Studies performed on different power system models illustrate the effectiveness of the strategy.

The investigation performed in this work highlighted three key abilities of the NSGAII that make it a better choice for application to RPPs over classical optimization strategies. The NSGAII can treat objective functions independently, perform global searches for the optimal solution and use a mixture of control types.

The ability to handle objective functions independently is highly important to a power system planner. Using the NSGAII as an optimization strategy for the RPP completely removes the necessity of weighting and summing objectives together to create a single objective. A weighted sum methodology is not attractive as optimization results may be erroneous due to objectives being of different units. Instead, the NSGAII uses the concept of Pareto-optimality to discover a range of feasible solutions that depict trade-offs that most often occur between competing objectives. With these trade-off solutions, a system planner has the ability to determine the best solution to implement based on some other information not defined in the RPP.

As the costs of purchasing and installing reactive devices for system load increase can be enormous, any optimization technique that inherently performs local search techniques can lead to solutions that may cost an electrical utility significantly more money than is actually required. However, the NSGAII's ability to search for global optimal VAr source allocations ensures that the optimization algorithm does not necessarily get stuck on local optimal solutions. Due to this, a power utility can potentially save considerable amounts of money using the NSGAII for RPP.

The last attribute that makes the NSGAII a good choice for the RPP is its ability to use a mixture of control parameter types. As the NSGAII works on the encoding of control parameters, the use of functional derivatives is not required for searching the problem space. The NSGAII does not require the approximation of discrete control parameters as continuous. Thus, the NSGAII further avoids sub-optimal solutions due to the rounding of each continuous control parameter to the nearest discrete value.

The three abilities of the NSGAII coupled with case study results presented make it possible to recommend the tool to electrical utilities as a potential means to solve the type of RPP used in this thesis.

It is important to note again that there is no guarantee that a solution obtained by the NSGAII is the true global solution for a particular RPP case study. This was evident from the case study presented in section 6.3 of this thesis. For this test case the results of three independent runs of the NSGAII resulted in two distinct Pareto-optimal solutions. Variable solution convergence is an attribute that must be accepted when using a heuristic optimization tool such as the NSGAII. However, the NSGAII can still be recommended as a RPP tool as it overcomes many of the limitations of classical optimization techniques.

7.1 Summary of the Research and Contribution of the Thesis

The main contributions of this thesis can be summarized as follows:

1. A complete analysis on the negative effects of reactive power transmission and the use of shunt reactive compensation devices to mitigate these effects.
2. A detailed study on reactive power planning problems, including important aspects such as its objectives and required operational constraints.

3. An investigation into binary GAs including their applicability to power system optimization problems.
4. Publication of technical paper [25] related to the application of GA methodologies to power system optimal power flow.
5. An overview of the Pareto-optimality concept that highlighted important implications of true multi-objective optimization.
6. The development of a MATLAB software tool based on the NSGAII for handling MOP objectives independently.
7. The application of the NSGAII software to two power system case studies highlighting the effectiveness of the heuristic strategy for overcoming the challenges associated with the RPP formulation.

7.2 Recommendations for Future Work

The NSGAII provide excellent quantitative and qualitative insight into the optimal allocation of VAr sources. However, it is impossible to say that the NSGAII technique will perform well for power systems of larger size that are operating under difficult conditions. As a result, further application of the tool to practical power systems under different operating conditions must be performed to increase its validation.

The GA parameters used in the case studies presented in this thesis were all chosen based on typical values found in GA literature. However, a minimal investigation

into how different GA parameter settings affect the NSGAII's output solution was performed. A study into the effects of different GA parameter settings is recommended as it may lead to the fine-tuning of the NSGAII, which may provide better solutions for RPPs.

On-going research into the use of multi-objective evolutionary strategies for solving RPPs indicates that no general strategy has been widely accepted to solve RPPs. Further, new research into multi-objective evolutionary strategies is constantly leading to new tool sets that outperform their predecessors. It is advised to investigate alternative evolutionary methodologies for application to RPPs in order to better gauge the capability of the NSGAII based RPP strategy. Alternative evolutionary strategies should include particle swarm algorithms and evolutionary algorithms.

This research focused solely on the use of binary based GAs. Some research has pointed out that continuous or integer encoded GAs can outperform binary GAs for specific problem applications [29]. Investigations into the benefits of using different encoding methods or even a mixture of encoding types should be done in order to possibly improve the performance of the NSGAII for solving RPPs.

Power systems should be able to operate without violating operational constraints after any possible single line outage [14]. In order to increase the practical quality of the solutions obtained by the NSGAII, only solutions that do not violate any operational constraint upon any single line outage should be considered feasible. An investigation into NSGAII's ability to recognize these solutions should be undertaken.

References

[1] U.S.-Canada Power System Outage Task Force. "Final Report on the August 14th Blackout." [cited 1 December 2006]. https://reports.energy.gov/

[2] P. Kundur, *Power System Stability and Control.* New York, NY: McGraw Hill, 1994.

[3] L. L. Lai, *Intelligent System Applications in Power Engineering: Evolutionary Programming and Neural Networks.* Chester, London: Wiley, 1998.

[4] W. Zhang, L. M. Tolbert, "Survey of Reactive Power Planning Methods," *IEEE Power Engineering Society General Meeting*, 12-16 June 2005, vol. 2, pp. 1430-1440.

[5] B. Baran, J. Vallejos, R. Ramos, U. Fernandex, "Multi-Objective Reactive Power Compensation," *IEEE/PES Transmission and Distribution Conference and Exposition*, 28 Oct. – 2 Nov. 2001, vol. 1, pp. 97-101.

[6] K. Iba, H. Suzuki, K. Suzuki, K. Suzuki, "Practical Reactive Power Allocation/Operation Planning Using Successive Linear Programming," *IEEE Trans. Power Syst.*, vol. 3, no. 2, pp. 558-566, 1988.

[7] J. A. Jatau, J. A. Momoh; A.U. Chuku, "Evaluation of Methodologies for Shunt Var Planning," *Proceedings on the Twenty-Second Annual North American Power Symposium*, 15-16 Oct. 1990, pp. 381-389.

[8] W. M. Lebow, R. Rouhani, R. Nadira, P. B. Uscoro, R. K. Mehra, D. W. Sobieski, M. K. Pal, M. P. Bhavaraju, "A Hierarchical Approach to Reactive Volt Ampere (Var) Optimization in System Planning," *IEEE Trans. on PAS*, vol. PAS-104, no. 8, pp 2051-2057, 1985.

[9] S. Granville, M. V. F. Pereira, A. Monticelli, "An Integrated Methodology for Var Source Planning," *IEEE Trans. Power Syst.*, vol. 3, no. 2, pp. 549-557, 1988.

[10] M. M Begovic, B. Radibratovic, F. C. Lambert, "On Multiobjective Volt-VAR Optimization in Power Systems," *Proceedings on the 37th Annual Hawaii International Conference on System Sciences*, 5-8 Jan. 2004, pp. 1-6.

[11] K. Y Lee, F.F Yang, "Optimal reactive power planning using evolutionary algorithms: a comparative study for evolutionary programming, evolutionary strategy, genetic algorithm, and linear programming," *IEEE Trans. on Power Syst.*, vol. 13, no. 1, pp 101-108, 1998.

[12] S. C. Chapra, R. P. Canale, *Numerical Methods for Engineers*. Boston, MA: McGraw-Hill, 1998.

[13] D. B. Fogel, Z. Michalewicz, *How to solve it: Modern Heuristics*, NewYork, NY, Springer, 2004.

[14] C. W. Taylor, *Power System Voltage Stability*. New York, NY: McGraw Hill, 1994.

[15] The MathWorks, Inc. "Multi-objective Optimization." [cited 10 November 2006]. http://www.mathworks.com/access/helpdesk/help/toolbox/optim/

[16] H. Saadat, *Power System Analysis*. Boston, MA: McGraw Hill, 2002.

[17] R. E Miller, *Optimization: Foundations and Applications*. New York, NY: Wiley 2000.

[18] M. Shahidehpour, Y. Fu. "Tutorial: Benders Decomposition in Restructured Power Systems" [cited 1 December 2006]. http://motor.ece.iit.edu/ms/benders.pdf

[19] J. H. Holland, "Genetic Algorithms." Iowa State University. [cited 5 September 2006]. http://www.econ.iastate.edu/tesfatsi/holland.GAIntro.htm

[20] D. E. Goldberg, *Genetic Algorithms in Search, Optimization and Machine Learning*. Reading, MA: Addison-Wesley, 1989.

[21] B. F. Wollenberg, A. J Wood, *Power Generation Operation and Control*. New York, NY: Wiley, 2000.

[22] M. Mitchell, *An Introduction to Genetic Algorithms*. Cambridge, MA: MIT Press, 1997.

[23] "Crossover Information." Answers.com. [cited 5 September 2006]. http://www.answers.com/topic/crossover-genetic-algorithm

[24] Matlab Version 7.1, MathWorks Inc., USA.

[25] S. M. Small, B. Jeyasurya, "Genetic Algorithms: Overview and Application to Power System Optimization," *16th Annual Newfoundland Electrical and Computer Engineering Conference*, November 9th 2006, St. John's Newfoundland.

[26] A. G. Bakirtzis, P. N. Biskas, C. E. Zoumas, V. Petridis, "Optimal Power Flow By Enhanced Genetic Algorithm," *IEEE Trans. Power Syst.*, vol. 17, no. 2, pp. 229-236, 2002.

[27] PowerWorld Simulator Version 12. PowerWorld Corporation, USA.

[28] R.D. Zimmerman, C.E. Murillo-Sánchez, D. Gan, "MATPOWER, a Matlab Power System Simulation Package," August 2005 http://www.pserc.cornell.edu/matpower/

[29] K. Deb, A. Pratap, S. Agarwal, T. Meyarivan, "A Fast and Elitist Multiobjective Genetic Algorithm: NSGA-II," *IEEE Transactions on Evolutionary Computation*, vol.6, no. 2, pp 182-197, 2002.

[30] K. Deb, *Multi-Objective Optimization using Evolutionary Algorithms*. New York, NY: Wiley, 2001.

[31] E. Zitzler, L. Thiele, "Multiobjective evolutionary algorithms: a comparative case study and the strength Pareto approach," *IEEE Transactions on Evolutionary Computation*, vol. 6, no. 4, pp. 257-271, 1999.

[32] J. Knowles, D. Corne, "The Pareto Archived Evolution Strategy: A New Baseline Algorithm for Pareto Multiobjective Optimisation," *Proceedings of the 1999 Congress on Evolutionary Computation*, 6-9 July 1999, pp. 98-105.

[33] S. M. Small, B. Jeyasurya, "Multi-Objective Reactive Power Planning: A Pareto Optimization Approach," Submitted to the *14th Annual Conference on Intelligent System Applications to Power Systems*, November 2007, Taiwan.

Appendix A: 7-Bus Power System Data

Appendix A gives contains the information about the 7-Bus Power System [27] discussed in the thesis. The single line diagram is shown in figure A.1. The line characteristics, generations, loads and generation fuel cost coefficients are presented in tables A.1, A.2, A.3 and A.4 respectively. Note that all bus voltages are required to be in the range of 0.95 p.u and 1.05 p.u.

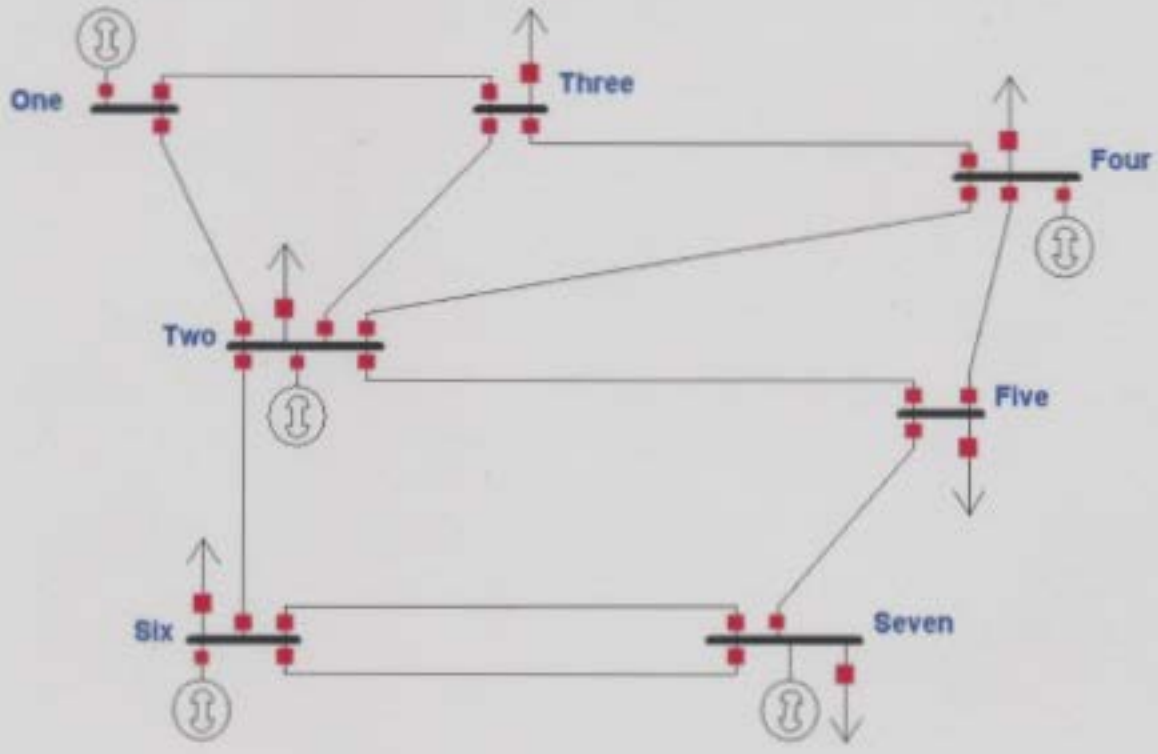

Figure A.1: One Line Diagram for the 7-Bus Power System

Table A.1: Line Characteristics for the 7-Bus System

Line No.	From Bus	To Bus	Resistance (p. u)	Reactance (p. u)	Line Charging (p. u)	Line Limit (MVA)
1	1	2	0.02	0.06	0.06	50
2	1	3	0.08	0.24	0.05	50
3	2	3	0.06	0.18	0.04	80
4	2	4	0.06	0.18	0.04	100
5	2	5	0.04	0.12	0.03	100
6	2	6	0.02	0.06	0.05	200
7	3	4	0.01	0.03	0.02	100
8	4	5	0.08	0.24	0.05	60
9	7	5	0.02	0.06	0.04	200
10	6	7	0.08	0.24	0.05	200
11	6	7	0.08	0.24	0.05	200

***All characteristics in p.u are based on 100MVA**

Table A.2: Generation Schedule and Generator Limits for the 7-Bus System

Bus	Active Power Generation (MW)	Maximum Active Power Generation (MW)	Minimum Active Power Generation (MW)	Maximum Reactive Power Generation (MVAr)	Minimum Reactive Power Generation (MVAr)
1	102	400	100	9900	-9900
2	170	500	150	9900	-9900
4	95	200	50	9900	-9900
6	200	500	150	9900	-9900
7	200.94	600	0	9900	-9900

Table A.3: Active and Reactive Load Demand for the 7-Bus System

Bus	Active Power Load (MW)	Reactive Power Load (MVAr)
2	40	20
3	110	40
4	80	30
5	130	40
6	200	0
7	200	0

Table A.4: Generator Fuel Cost Coefficients of the 7-Bus System

Bus	α	β	γ
1	373.5	7.62	0.002
2	403.61	7.519	0.0014
4	253.24	7.836	0.0013
6	388.93	7.573	0.0013
7	194.28	7.771	0.0019

Appendix B: 6-Bus Power System Data

Appendix B gives contains the pertinent information about the 6-Bus Power System [21] discussed in the thesis. The single line diagram is shown in figure B.1. The line characteristics, initial generation schedule and initial load demand are presented in tables B.1, B.2, and B.3. Note that all bus voltages are required to be in the range of 0.95 p.u and 1.05 p.u.

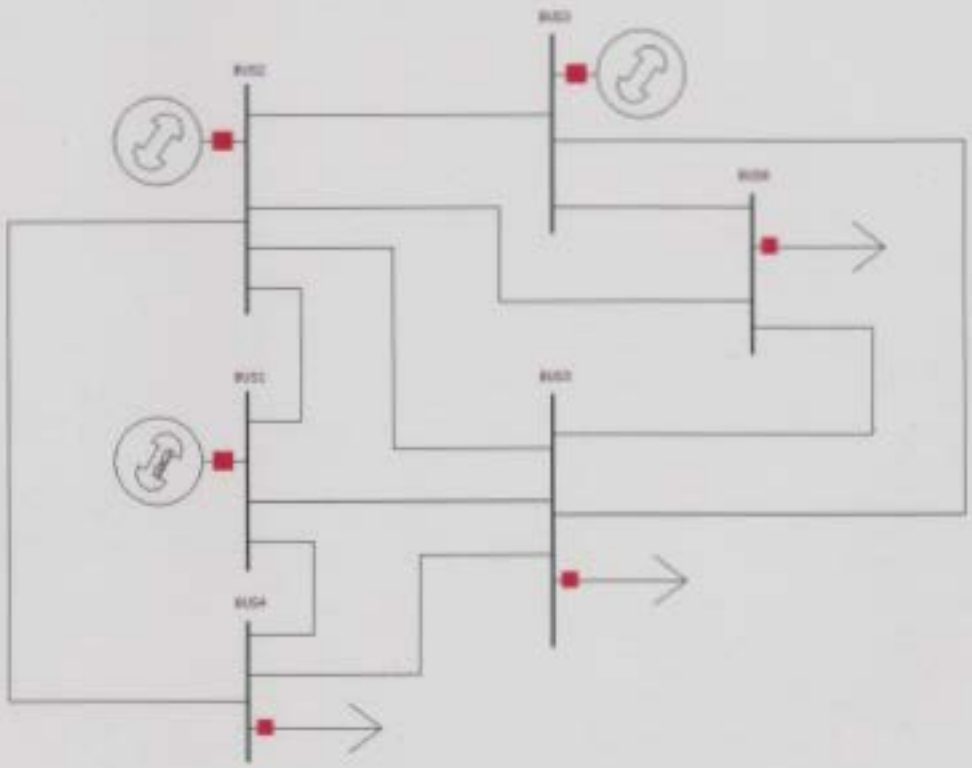

Figure B.1: Single Line Diagram of the 6-Bus Test System

Table B.1: Line Characteristics for the 6-Bus System

Line No.	From Bus	To Bus	Resistance (p. u)	Reactance (p. u)	Line Charging (p. u)	Line Limit (MVA)
1	1	2	0.1	0.2	0.02	100
2	1	4	0.05	0.2	0.02	100
3	1	5	0.08	0.3	0.03	100
4	2	3	0.05	0.25	0.03	100
5	2	4	0.05	0.1	0.01	100
6	2	5	0.1	0.3	0.02	100
7	2	6	0.07	0.2	0.025	100
8	3	5	0.12	0.26	0.025	100
9	3	6	0.02	0.1	0.01	100
10	4	5	0.2	0.4	0.04	100
11	6	5	0.1	0.3	0.03	100

***All characteristics in p.u are based on 100MVA**

Table B.2: Initial Generation Schedule and Generator Limits for the 6-Bus System

Bus	Active Power Generation (MW)	Maximum Active Power Generation (MW)	Minimum Active Power Generation (MW)	Maximum Reactive Power Generation (MVAr)	Minimum Reactive Power Generation (MVAr)
1	108.5	165	0	100	-10
2	50	165	30	100	-10
3	60	165	40	100	-10

Table B.3: Initial Active and Reactive Load Demand for the 6-Bus System

Bus	Active Power Load (MW)	Reactive Power Load (MVAr)
4	70	70
5	70	70
6	70	70

Appendix C: IEEE 30-Bus Power System Data

Appendix C gives contains the pertinent information about the IEEE 30-Bus Power System discussed in the thesis. The single line diagram is shown in figure C.1. The line characteristics, initial generation schedule and initial load demand including initial reactive compensation are presented in tables C.1, C.2, and C.3. Note that all bus voltages are required to be in the range of 0.95 p.u and 1.05 p.u.

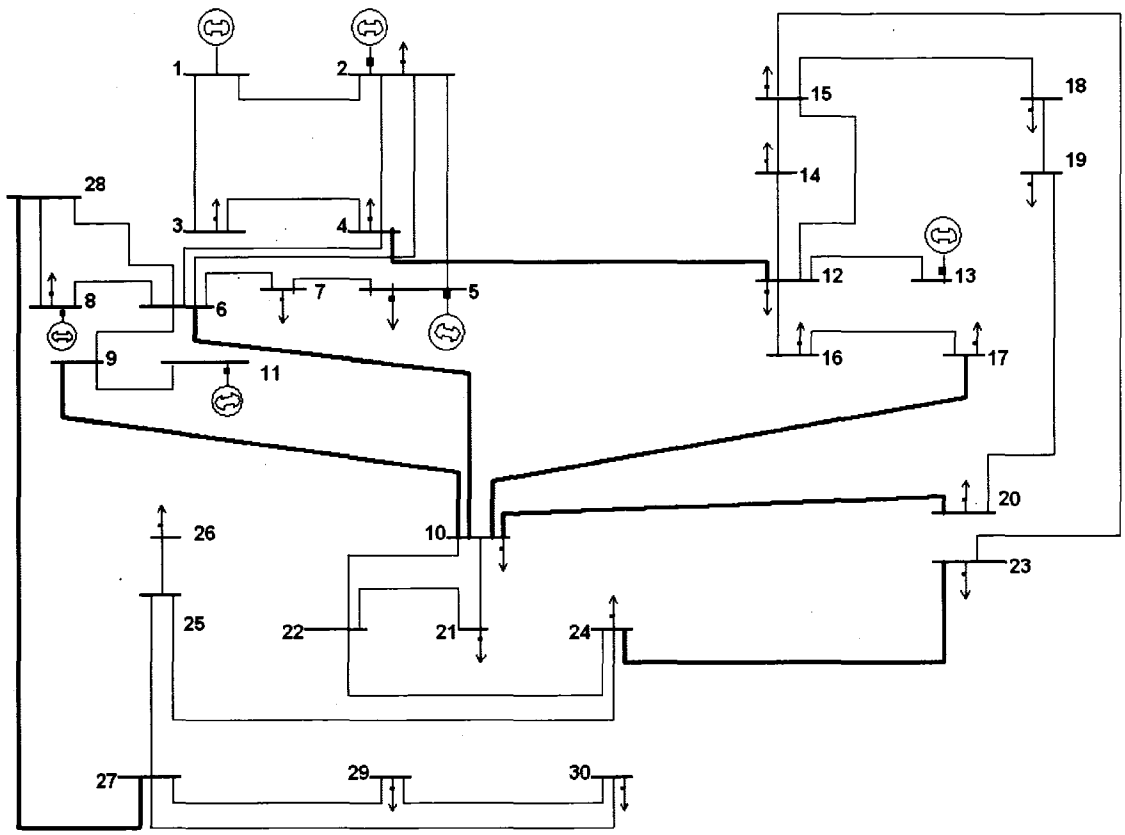

Figure C.1: One Line Diagram of the IEEE-30 Test System

Table C.1: Line Characteristics for the IEEE 30-Bus System

Line No.	From Bus	To Bus	Resistance (p. u)	Reactance (p. u)	Line Charging (p. u)	Line Limit (MVA)
1	1	2	0.0192	0.0575	0.0528	110
2	1	3	0.0452	0.1652	0.0408	110
3	2	4	0.057	0.1737	0.0368	110
4	3	4	0.0132	0.0379	0.0084	110
5	2	5	0.0472	0.1983	0.0418	110
6	2	6	0.0581	0.1763	0.0374	110
7	4	6	0.0119	0.0414	0.009	110
8	5	7	0.046	0.116	0.0204	110
9	6	7	0.0267	0.082	0.017	110
10	6	8	0.012	0.042	0.009	110
11	6	9	0	0.208	0	110
12	6	10	0	0.556	0	110
13	9	11	0	0.208	0	110
14	9	10	0	0.11	0	110
15	4	12	0	0.256	0	110
16	12	13	0	0.14	0	110
17	12	14	0.1231	0.2559	0	110
18	12	15	0.0662	0.1304	0	110
19	12	16	0.0945	0.1987	0	110
20	14	15	0.221	0.1997	0	110
21	16	17	0.0524	0.1923	0	110
22	15	18	0.1073	0.2185	0	110
23	18	19	0.0639	0.1292	0	110
24	19	20	0.034	0.068	0	110
25	10	20	0.0936	0.209	0	110
26	10	17	0.0324	0.0845	0	110
27	10	21	0.0348	0.0749	0	110
28	10	22	0.0727	0.1499	0	110
29	21	22	0.0116	0.0236	0	110
30	15	23	0.1	0.202	0	110
31	22	24	0.115	0.179	0	110
32	23	24	0.132	0.27	0	110
33	24	25	0.1885	0.3292	0	110
34	25	26	0.2544	0.38	0	110

35	25	27	0.1093	0.2087	0	110
36	28	27	0	0.396	0	110
37	27	29	0.2198	0.4153	0	110
38	27	30	0.3202	0.6027	0	110
39	29	30	0.2399	0.4533	0	110
40	8	28	0.0636	0.2	0.0428	110
41	6	28	0.0169	0.0599	0.013	110

***All characteristics in p.u are based on 100MVA**

Table C.2: Initial Generation Schedule and Generator Limits for the IEEE 30-Bus System

Bus	Active Power Generation (MW)	Maximum Active Power Generation (MW)	Minimum Active Power Generation (MW)	Maximum Reactive Power Generation (MVAr)	Minimum Reactive Power Generation (MVAr)
1	87.56	100	0	150	-20
2	40	140	0	60	-20
5	40	100	0	62.5	-15
8	40	100	0	48.7	-15
11	40	100	0	40	-10
13	40	100	0	44.7	-15

Table C.3: Initial Active and Reactive Load Demand for the IEEE 30-Bus System

Bus	Active Power Load (MW)	Reactive Power Load (MVAr)	Reactive Power Injection (MVAr at 1.0 p.u voltage)
2	21.7	12.7	0
3	2.4	1.2	0
4	7.6	1.6	0
5	94.2	19	0
6	0	0	0
7	22.8	10.9	0
8	30	30	0
9	0	0	0
10	5.8	2	19

12	11.2	7.5	0
14	6.2	1.6	0
15	8.2	2.5	0
16	3.5	1.8	0
17	9	5.8	0
18	3.2	0.9	0
19	9.5	3.4	0
20	2.2	0.7	0
21	17.5	11.2	0
22	0	0	0
23	3.2	1.6	0
24	8.7	6.7	4.3
25	0	0	0
26	3.5	2.3	0
27	0	0	0
28	0	0	0
29	2.4	0.9	0
30	10.6	1.9	0